Geometry and dynamics in moduli spaces

Lecture 9. Idea of renormalization. Windtree model. Lyapunov exponents

Anton Zorich
Université Paris Cité

March 31, 2026

“You, my forest and water! One swerves, while the other shall spout
Through your body like draught; one declares, while the first has a doubt.”
J. Brodsky

Ты, мой лес и вода, кто обгедет, а кто, как сквозняк,
проникает в тебя, кто глаголет, а кто обиняк...
И. Бродский

Periodic billiards

Central limit theorem

Let $X_1, ..., X_n$ be a sequence of independent and identically distributed random variables (heads or tails, measurements in uncorrelated experiments, etc). Assume that the variance σ^2 is finite and that the expected value is 0. Let $S_n := X_1 + \cdots + X_n$. Clearly, with probability one one has

$$\frac{X_1 + \cdots + X_n}{n} = \frac{S_n}{n} \to 0 \quad \text{as } n \to +\infty\,.$$

The Central Limit Theorem describes the expected deviation of the sum S_n from 0. In a sense, it is one of the fundamental laws of Nature:

Cental Limit Theorem. *The distribution of the the sum S_n normalized by the factor $\frac{1}{\sqrt{n}}$ tends to the normal distribution with mean 0 and variance σ^2.*

Random walk and brownian motion in the plane

Random walk. For every step you flip two coins; depending of the combination you go one step forward, one step backward, one step right, or one step left.

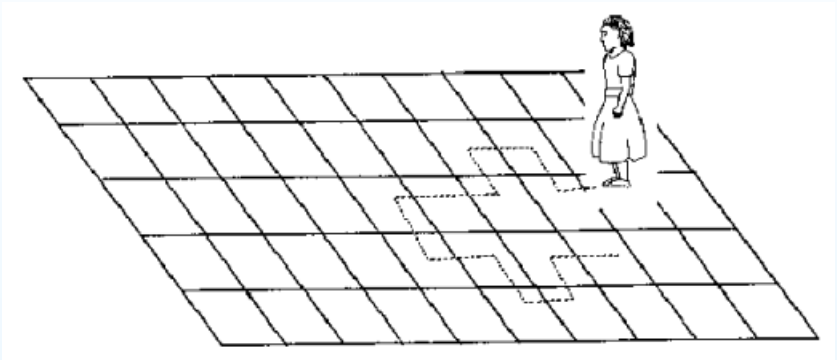

Random walk and brownian motion in the plane

Random walk. For every step you flip two coins; depending of the combination you go one step forward, one step backward, one step right, or one step left.

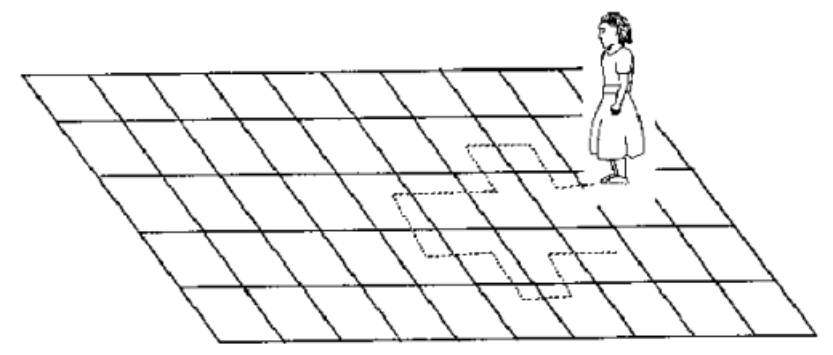

Corollary of the Central Limit Theorem. *The root of the mean square of the translation distance after n steps of a random walk with zero mean is*

$$\sqrt{E|S_n^2|} = \sigma\sqrt{n} = \sigma \cdot n^{\frac{1}{2}} .$$

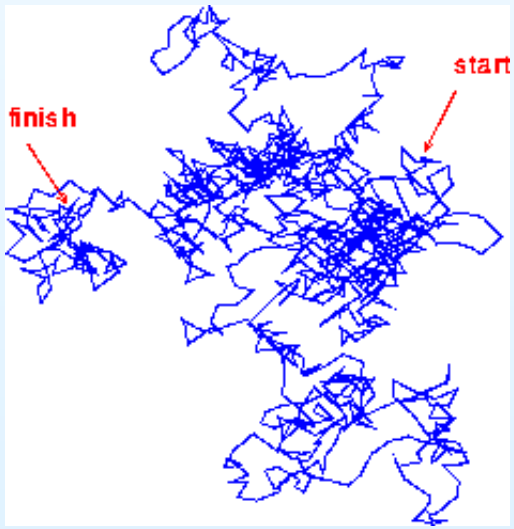

Lorentz gas and Sinai billiard. Finite horizon.

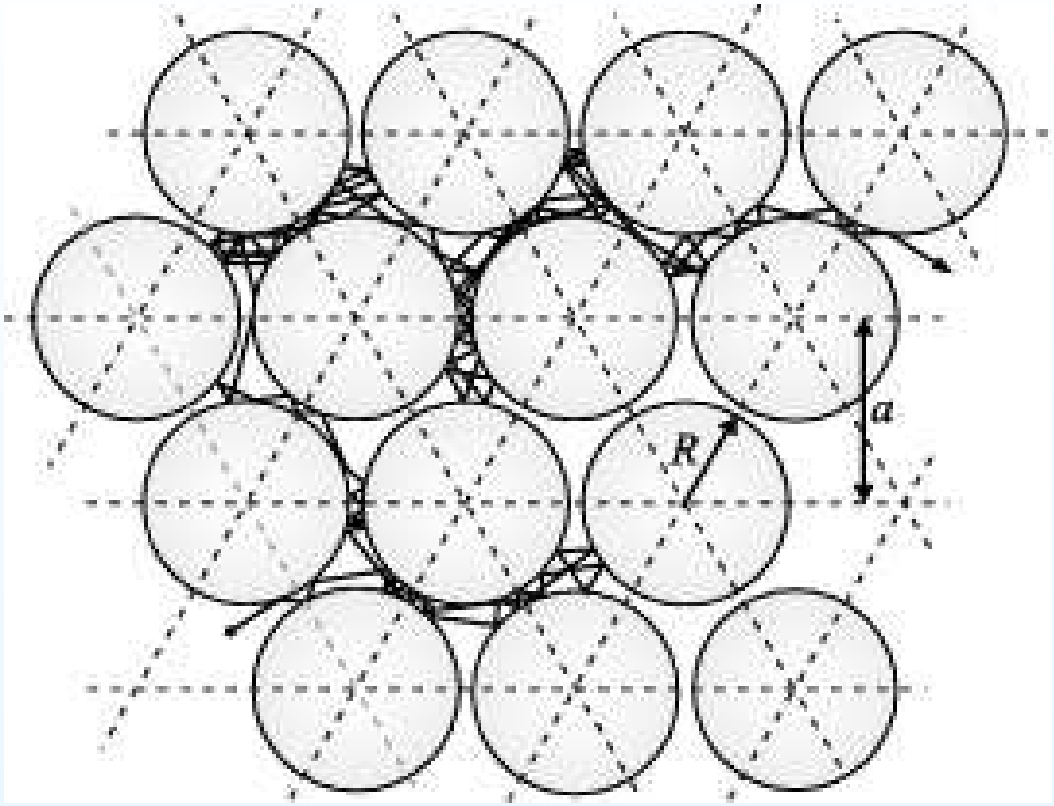

Theorem (Bunimovich, Chernov, Sinai, 1991). *For periodic configuration of convex scatterers on the plane the particle after scaling by $\sqrt{t}$ satisfies the Central Limit Theorem if the horizon is finite (that is, if any ray intersects a scatterer).*

Lorentz gas and Sinai billiard. Infinite horizon.

Theorem (Szász, Varjú, 2007; some ideas — Bleher, 1992).
In infinite horizon case, for example, for round scatterers placed at the lattice points, the Central Limit Theorem still holds but the scaling should be by $\sqrt{t \ln t}$.

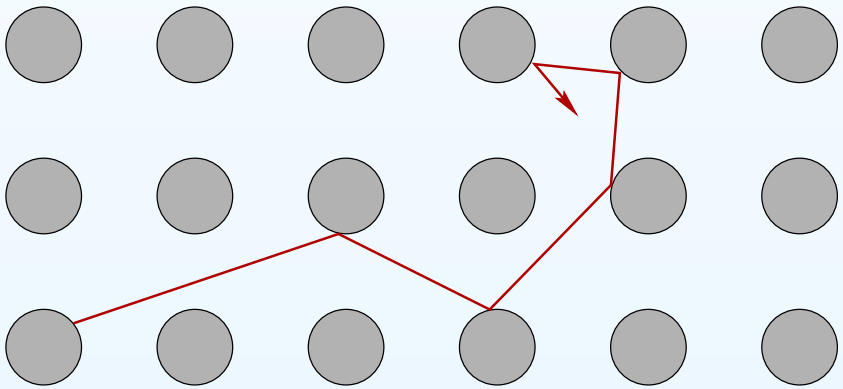

Chernov, Dolgopyat (2009): further interesting results in this direction.

In all cases the *diffusion rate* is again $\frac{1}{2}$ as for the random walk.

Diffusion in a periodic billiard (Ehrenfest “Windtree model”)

Consider a billiard on the plane with $\mathbb{Z}^2$-periodic rectangular obstacles.

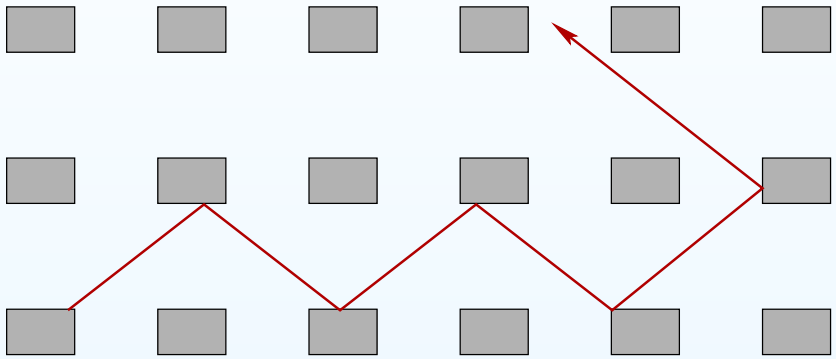

Theorem (V. Delecroix, P. Hubert, S. Lelièvre, 2014). *For all parameters of the obstacle, for almost all initial directions, and for any starting point, the billiard trajectory spreads in the plane with the speed $\sim t^{2/3}$. That is,*

$$\lim_{t\to+\infty} \log(\text{diameter of trajectory of length } t)/\log t = \tfrac{2}{3} \neq \tfrac{1}{2}.$$

The diffusion rate $\frac{2}{3}$ is given by the Lyapunov exponent of certain renormalizing dynamical system associated to the initial one.

Remark. Changing the height and the width of the obstacle we get quite different billiards, but this does not change the diffusion rate!

Diffusion in a periodic billiard (Ehrenfest “Windtree model”)

Consider a billiard on the plane with $\mathbb{Z}^2$-periodic rectangular obstacles.

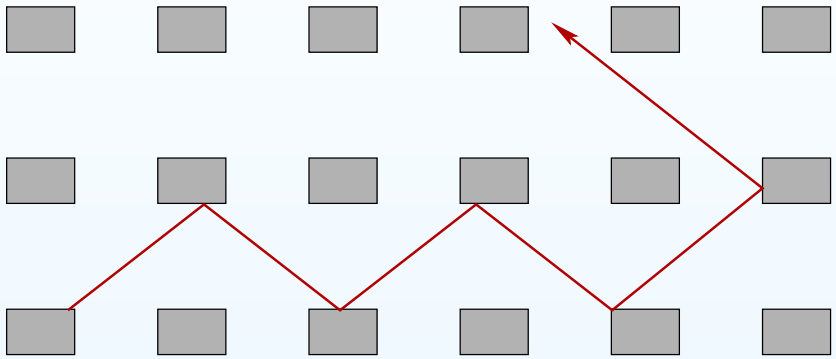

Theorem (V. Delecroix, P. Hubert, S. Lelièvre, 2014). *For all parameters of the obstacle, for almost all initial directions, and for any starting point, the billiard trajectory spreads in the plane with the speed $\sim t^{2/3}$. That is,*

$$\lim_{t\to+\infty} \log(\text{diameter of trajectory of length } t)/\log t = \tfrac{2}{3} \neq \tfrac{1}{2}.$$

The diffusion rate $\frac{2}{3}$ is given by the Lyapunov exponent of certain renormalizing dynamical system associated to the initial one.

Remark. Changing the height and the width of the obstacle we get quite different billiards, but this does not change the diffusion rate!

Diffusion in a periodic billiard (Ehrenfest “Windtree model”)

Consider a billiard on the plane with $\mathbb{Z}^2$-periodic rectangular obstacles.

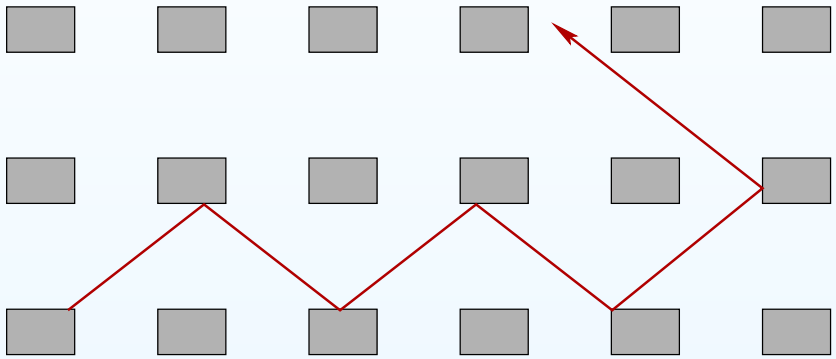

Theorem (V. Delecroix, P. Hubert, S. Lelièvre, 2014). *For all parameters of the obstacle, for almost all initial directions, and for any starting point, the billiard trajectory spreads in the plane with the speed $\sim t^{2/3}$. That is,*

$$\lim_{t\to+\infty} \log(\text{diameter of trajectory of length } t)/\log t = \tfrac{2}{3} \neq \tfrac{1}{2}.$$

The diffusion rate $\frac{2}{3}$ is given by the Lyapunov exponent of certain renormalizing dynamical system associated to the initial one.

Remark. Changing the height and the width of the obstacle we get quite different billiards, but this does not change the diffusion rate!

Diffusion in a periodic billiard (Ehrenfest “Windtree model”)

Consider a billiard on the plane with $\mathbb{Z}^2$-periodic rectangular obstacles.

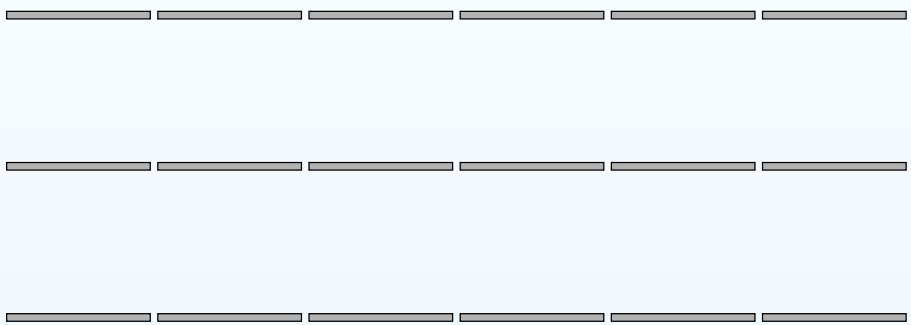

Theorem (V. Delecroix, P. Hubert, S. Lelièvre, 2014). *For all parameters of the obstacle, for almost all initial directions, and for any starting point, the billiard trajectory spreads in the plane with the speed $\sim t^{2/3}$. That is,*

$$\lim_{t\to+\infty} \log(\text{diameter of trajectory of length } t)/\log t = \tfrac{2}{3} \neq \tfrac{1}{2}.$$

The diffusion rate $\frac{2}{3}$ is given by the Lyapunov exponent of certain renormalizing dynamical system associated to the initial one.

Remark. Changing the height and the width of the obstacle we get quite different billiards, but this does not change the diffusion rate!

Diffusion in a periodic billiard (Ehrenfest “Windtree model”)

Consider a billiard on the plane with $\mathbb{Z}^2$-periodic rectangular obstacles.

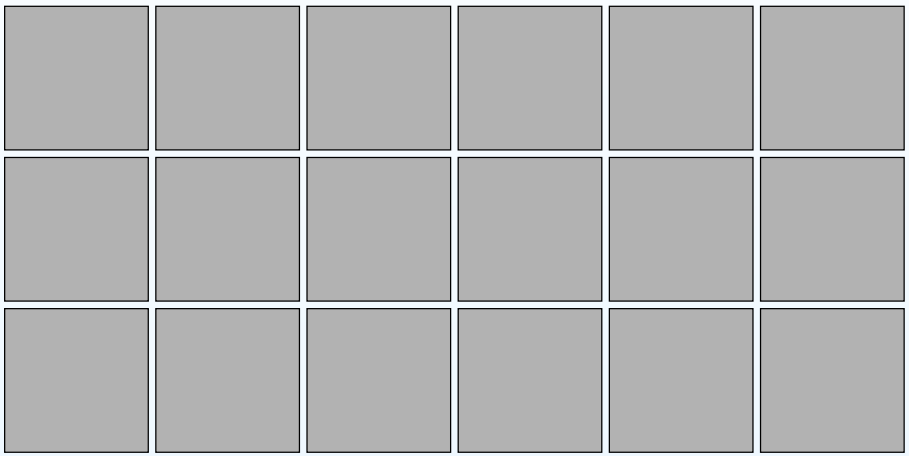

Theorem (V. Delecroix, P. Hubert, S. Lelièvre, 2014). *For all parameters of the obstacle, for almost all initial directions, and for any starting point, the billiard trajectory spreads in the plane with the speed $\sim t^{2/3}$. That is,*

$$\lim_{t\to+\infty} \log(\text{diameter of trajectory of length } t)/\log t = \tfrac{2}{3} \neq \tfrac{1}{2}.$$

The diffusion rate $\frac{2}{3}$ is given by the Lyapunov exponent of certain renormalizing dynamical system associated to the initial one.

Remark. Changing the height and the width of the obstacle we get quite different billiards, but this does not change the diffusion rate!

From billiards to surface foliations

Consider a rectangular billiard. Instead of reflecting the trajectory we can reflect the billiard table. The trajectory unfolds to a straight line. Folding back the copies of the billiard table we project this line to the original trajectory. At any moment the ball moves in one of four directions defining four types of copies of the billiard table. Copies of the same type are related by a parallel translation.

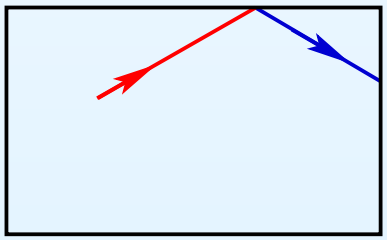

From billiards to surface foliations

Consider a rectangular billiard. Instead of reflecting the trajectory we can reflect the billiard table. The trajectory unfolds to a straight line. Folding back the copies of the billiard table we project this line to the original trajectory. At any moment the ball moves in one of four directions defining four types of copies of the billiard table. Copies of the same type are related by a parallel translation.

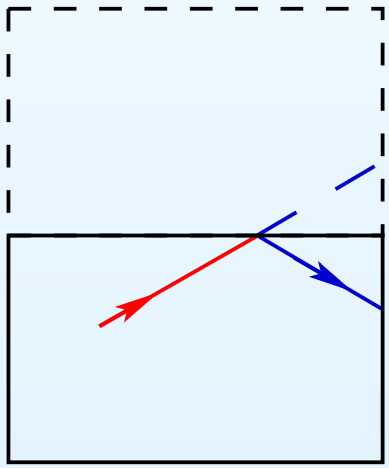

From billiards to surface foliations

Consider a rectangular billiard. Instead of reflecting the trajectory we can reflect the billiard table. The trajectory unfolds to a straight line. Folding back the copies of the billiard table we project this line to the original trajectory. At any moment the ball moves in one of four directions defining four types of copies of the billiard table. Copies of the same type are related by a parallel translation.

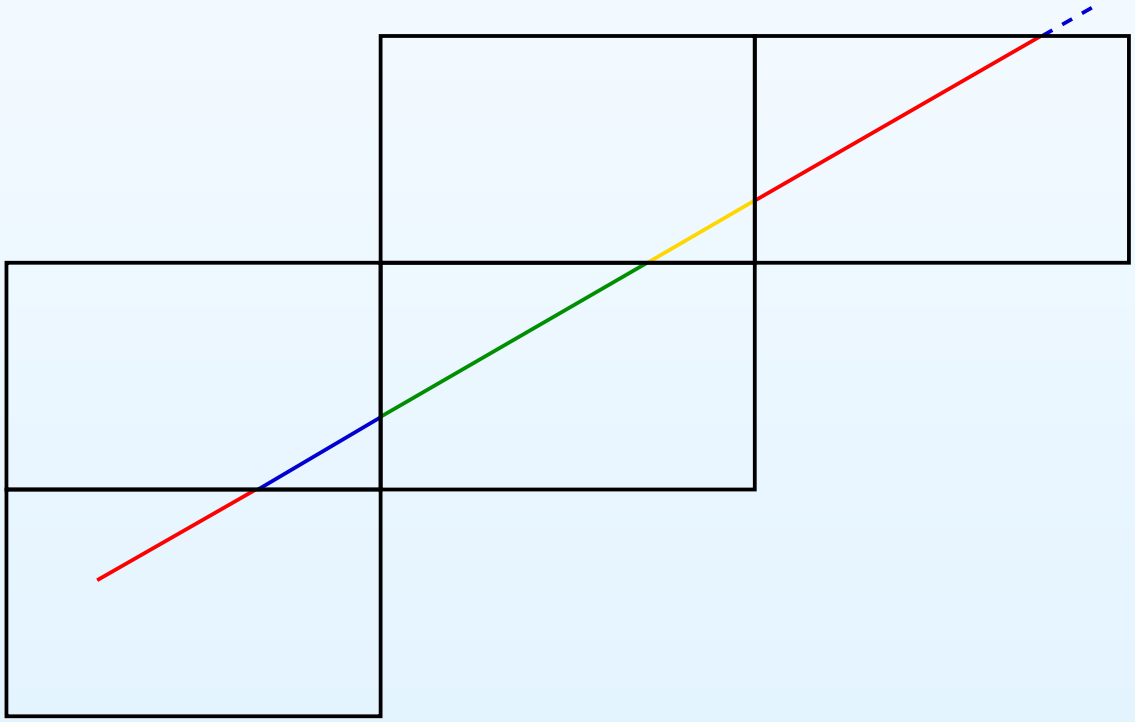

From billiards to surface foliations

Consider a rectangular billiard. Instead of reflecting the trajectory we can reflect the billiard table. The trajectory unfolds to a straight line. Folding back the copies of the billiard table we project this line to the original trajectory. At any moment the ball moves in one of four directions defining four types of copies of the billiard table. Copies of the same type are related by a parallel translation.

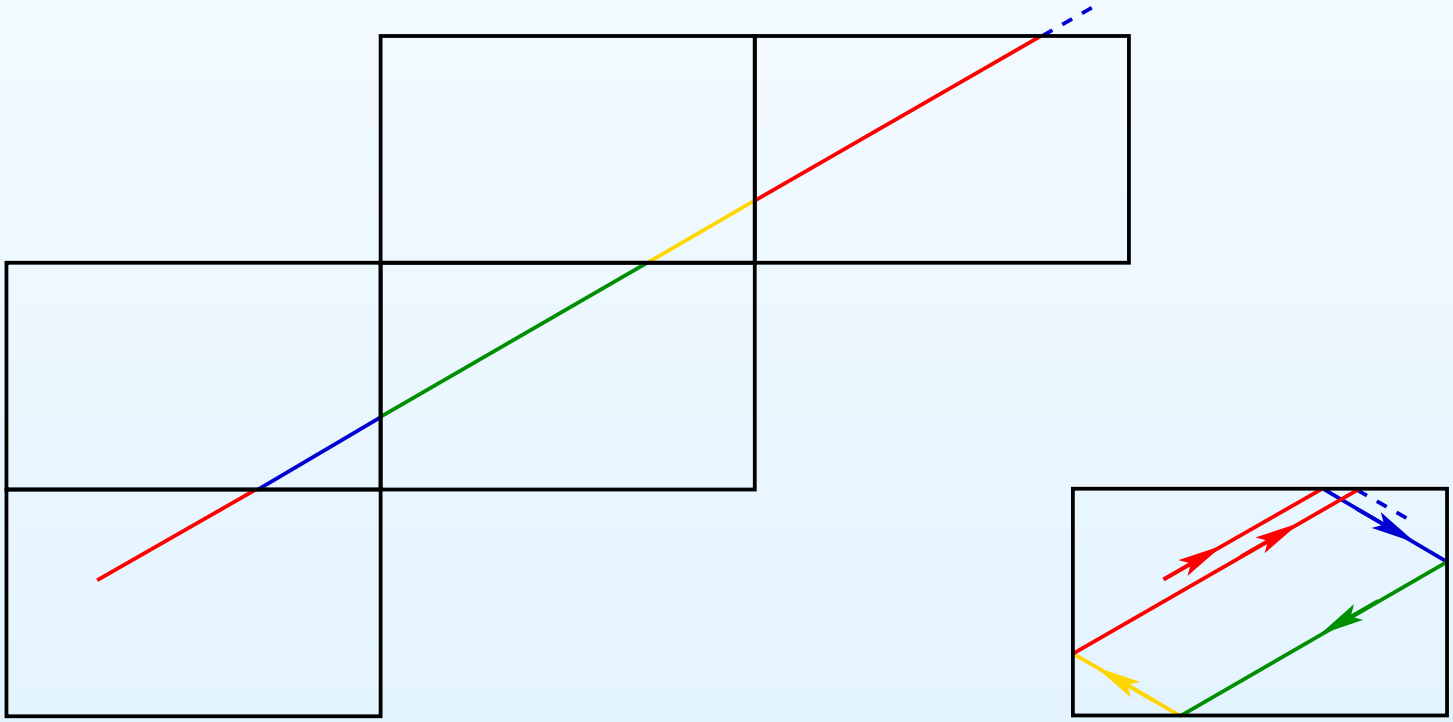

From billiards to surface foliations

Consider a rectangular billiard. Instead of reflecting the trajectory we can reflect the billiard table. The trajectory unfolds to a straight line. Folding back the copies of the billiard table we project this line to the original trajectory. At any moment the ball moves in one of four directions defining four types of copies of the billiard table. Copies of the same type are related by a parallel translation.

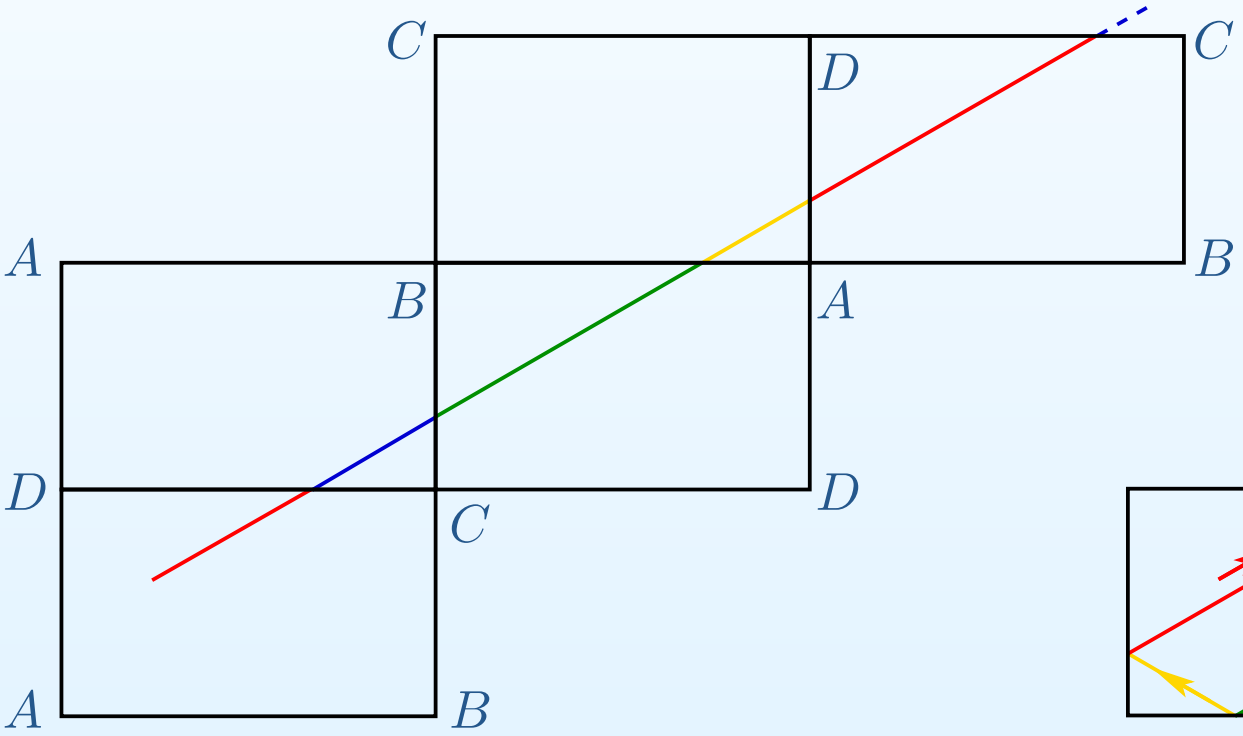

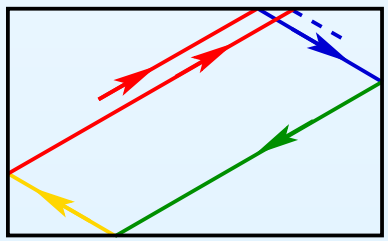

From billiards to surface foliations

Consider a rectangular billiard. Instead of reflecting the trajectory we can reflect the billiard table. The trajectory unfolds to a straight line. Folding back the copies of the billiard table we project this line to the original trajectory. At any moment the ball moves in one of four directions defining four types of copies of the billiard table. Copies of the same type are related by a parallel translation.

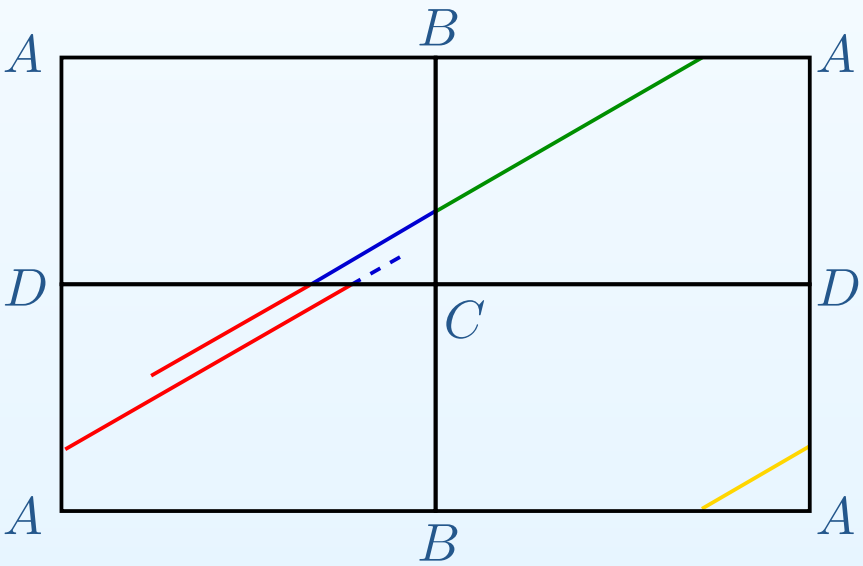

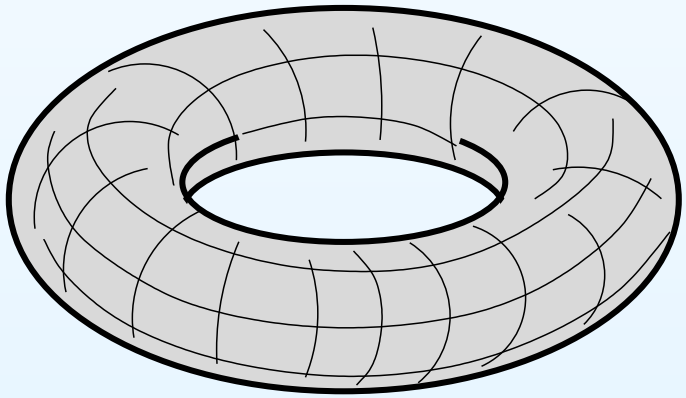

Identifying the equivalent patterns by a parallel translation we obtain a torus; the billiard trajectory unfolds to a “straight line” on the corresponding torus.

From billiards to surface foliations

Consider a rectangular billiard. Instead of reflecting the trajectory we can reflect the billiard table. The trajectory unfolds to a straight line. Folding back the copies of the billiard table we project this line to the original trajectory. At any moment the ball moves in one of four directions defining four types of copies of the billiard table. Copies of the same type are related by a parallel translation.

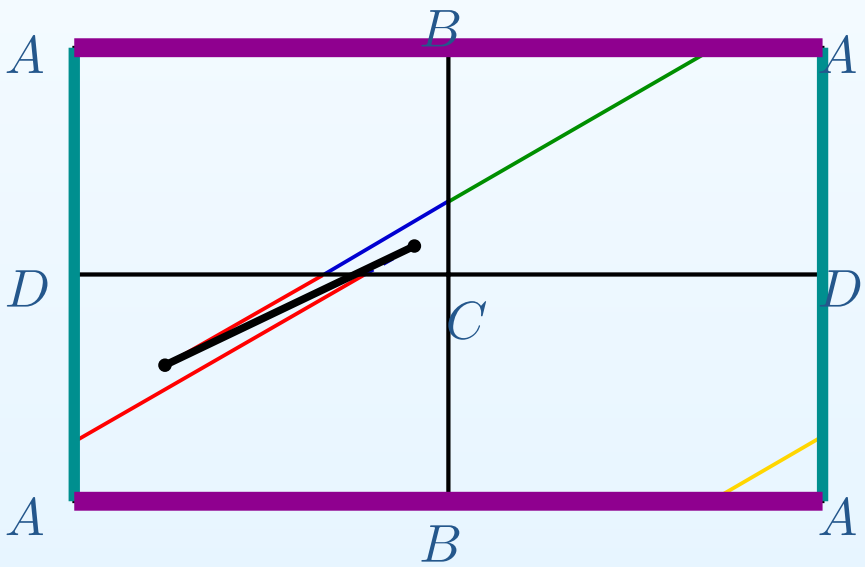

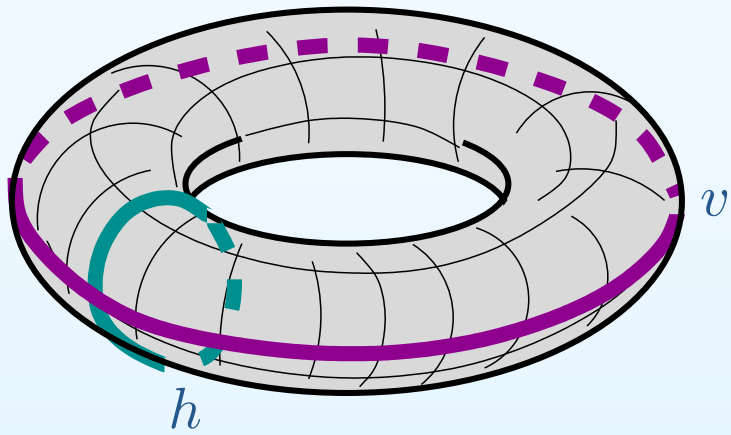

Join the endpoints of a piece of trajectory after time t to obtain a closed loop $c(t)$ on the torus. Vertical and horizontal displacement after time t of the unfolded billiard trajectory is described by the intersection numbers $c(t) \circ h$ and $c(t) \circ v$ with a parallel h and a meridian v of the torus.

Windtree flat surface

Similarly, taking four copies of our $\mathbb{Z}^2$-periodic windtree billiard we can unfold it to a foliation on a $\mathbb{Z}^2$-periodic surface. Taking a quotient over $\mathbb{Z}^2$ we get a compact surface endowed with a measured foliation. Vertical and horizontal displacement (and thus, the diffusion) of billiard trajectories is described by the intersection numbers $c(t) \circ h$ and $c(t) \circ v$ of the cycle $c(t)$ obtained by closing up a long piece of leaf with a "parallel" h and a "meridian" v. Here $h = h_{00} + h_{10} - h_{01} - h_{11}$ and $v = v_{00} - v_{10} + v_{01} - v_{11}$.

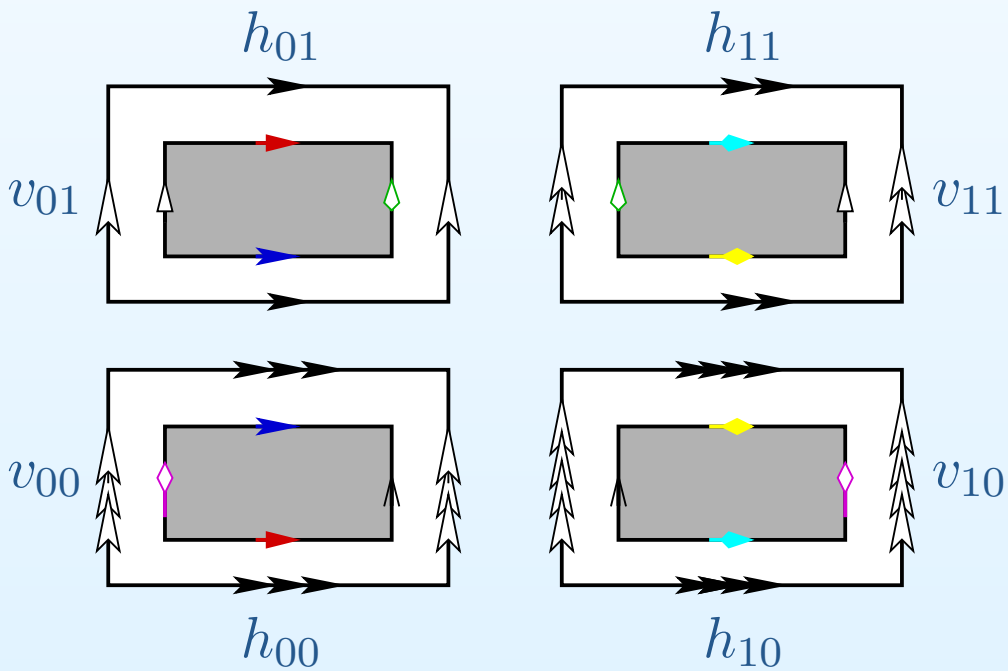

Motivation to study billiards: gas of two molecules in a one-dimensional chamber

Consider two elastic balls (“molecules”) sliding along a rod. They are bounded from two sides by solid walls. All collisions are ideal — without loss of energy.

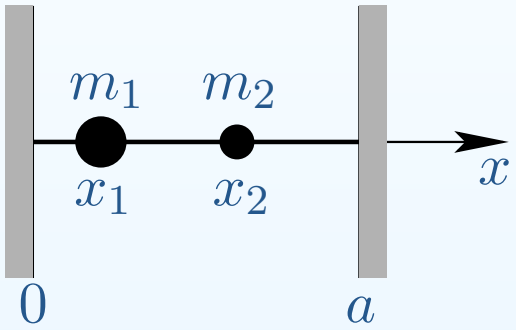

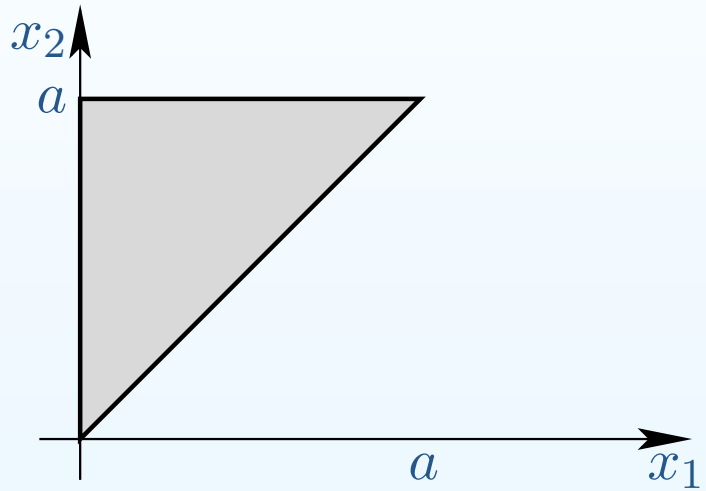

Motivation to study billiards: gas of two molecules in a one-dimensional chamber

Consider two elastic balls (“molecules”) sliding along a rod. They are bounded from two sides by solid walls. All collisions are ideal — without loss of energy.

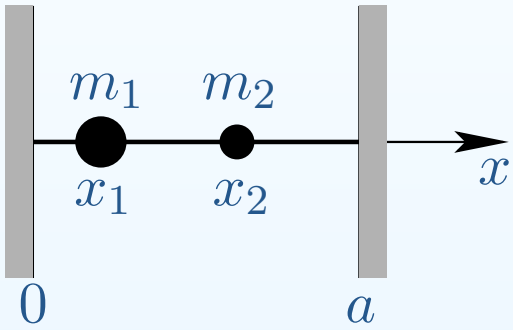

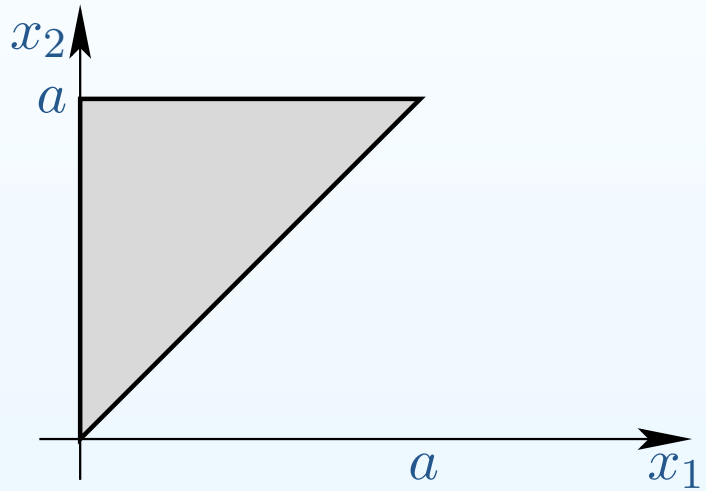

Neglecting the sizes of the balls we can describe the configuration space of our system using coordinates $0 < x_1 \leq x_2 \leq a$ of the balls, where a is the distance between the walls. This gives a right isosceles triangle.

Gas of two molecules

Rescaling the coordinates by square roots of masses

$$\begin{cases} \tilde{x}_1 &= \sqrt{m_1}x_1 \\ \tilde{x}_2 &= \sqrt{m_2}x_2 \end{cases}$$

we get a new right triangle Δ as a configuration space.

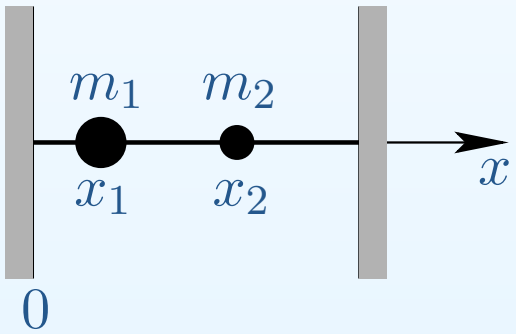

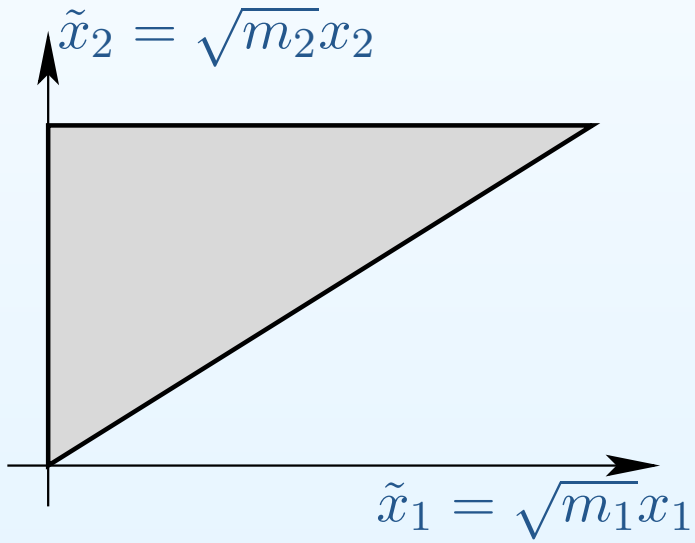

Gas of two molecules

Rescaling the coordinates by square roots of masses

$$\begin{cases} \tilde{x}_1 &= \sqrt{m_1}x_1 \\ \tilde{x}_2 &= \sqrt{m_2}x_2 \end{cases}$$

we get a new right triangle Δ as a configuration space.

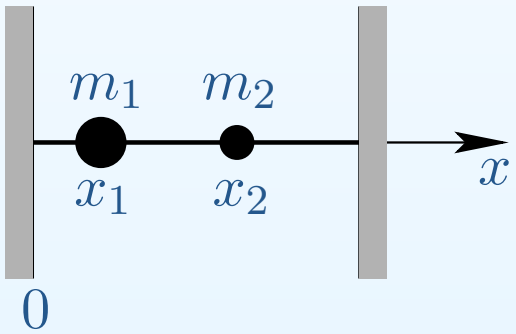

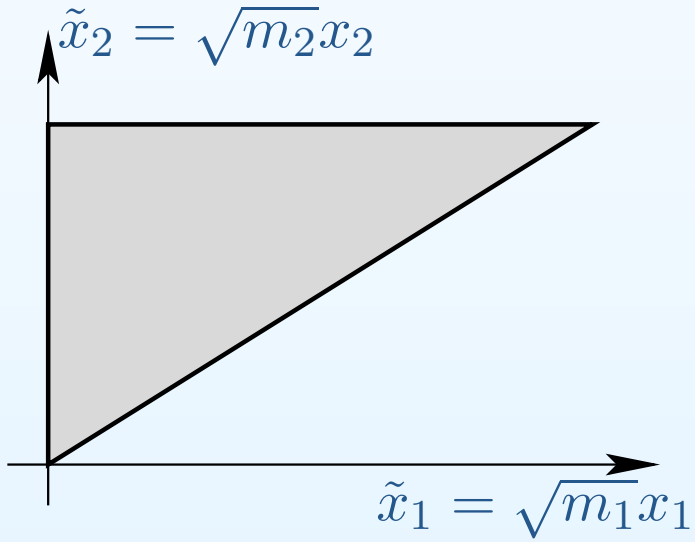

Lemma *In coordinates $(\tilde{x}_1, \tilde{x}_2)$ trajectories of the system of two balls on a rod correspond to billiard trajectories in the triangle Δ.*

Reminder: group action, Masur–Veech theorem, Magic Wand theorem

Group action

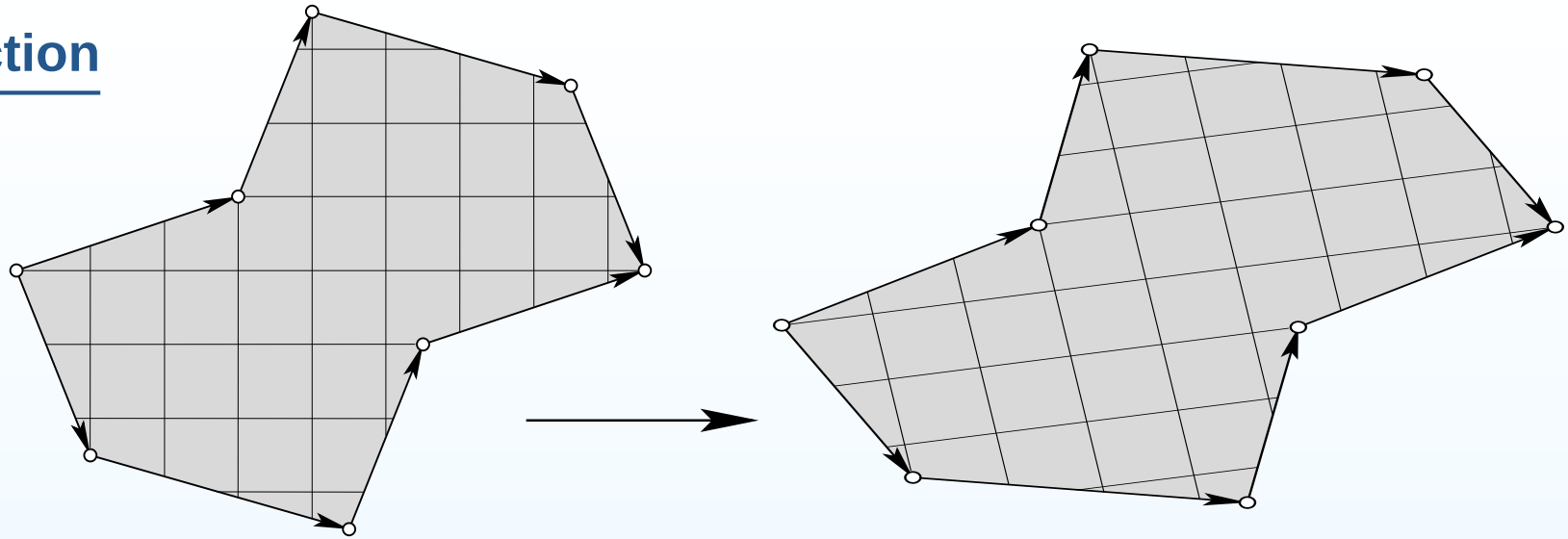

The subgroup $\mathrm{SL}(2,\mathbb{R})$ of area preserving linear transformations acts on the "unit hyperboloid" $\mathcal{H}_1(d_1,\ldots,d_n)$. The diagonal subgroup $\begin{pmatrix} e^t & 0 \\ 0 & e^{-t} \end{pmatrix} \subset SL(2,\mathbb{R})$ induces a natural flow on the stratum, which is called the *Teichmüller geodesic flow*.

Key Theorem (H. Masur; W. A. Veech) *The action of the groups $SL(2,\mathbb{R})$ and $\begin{pmatrix} e^t & 0 \\ 0 & e^{-t} \end{pmatrix}$ preserves the Masur–Veech measure. Both actions are ergodic with respect to this measure on each connected component of every stratum $\mathcal{H}_1(d_1,\ldots,d_n)$.*

Moduli spaces of Abelian differentials

We have seen that any stratum $\mathcal{H}(m_1, \dots, m_n)$ of all pairs
(Riemann surface S, holomorphic 1-form with n zeroes of degrees $m_1, \dots, m_n$)
is locally modeled on $H^1(S, \{n \text{ points}\}; \mathbb{C})$. The action of the group $\mathrm{GL}(2, \mathbb{R})$ can be seen as the action on the second term in the product

$$H^1(S, \{n \text{ points}\}; \mathbb{R} \oplus i\mathbb{R}) \simeq H^1(S, \{n \text{ points}\}; \mathbb{R}) \otimes \mathbb{R}^2 \,.$$

Moduli spaces of Abelian differentials

We have seen that any stratum $\mathcal{H}(m_1, \dots, m_n)$ of all pairs *(Riemann surface S, holomorphic 1-form with n zeroes of degrees $m_1, \dots, m_n$)* is locally modeled on $H^1(S, \{n \text{ points}\}; \mathbb{C})$. The action of the group $\mathrm{GL}(2, \mathbb{R})$ can be seen as the action on the second term in the product

$$H^1(S, \{n \text{ points}\}; \mathbb{R} \oplus i\mathbb{R}) \simeq H^1(S, \{n \text{ points}\}; \mathbb{R}) \otimes \mathbb{R}^2 \,.$$

A projectivized stratum $\mathrm{P}\mathcal{H}(m_1, \dots, m_n) \simeq \mathcal{H}_1(m_1, \dots, m_n)/\mathrm{SO}(2, \mathbb{R}) \simeq \mathcal{H}(m_1, \dots, m_n)/\mathbb{C}^*$ is foliated by hyperbolic planes $\mathbb{H}^2 = \mathrm{SL}(2, \mathbb{R})/\mathrm{SO}(2, \mathbb{R})$ called *Teichmüller discs*. A natural projection of such a disc to $\mathcal{M}_g$ is an isometric immersion with respect to Teichüller metric on $\mathcal{M}_g$, so Teichmüller discs can be seen as *complex geodesics* in the Teichmüller metric on $\mathcal{M}_g$.

Moduli spaces of Abelian differentials

We have seen that any stratum $\mathcal{H}(m_1, \dots, m_n)$ of all pairs *(Riemann surface S, holomorphic 1-form with n zeroes of degrees $m_1, \dots, m_n$)* is locally modeled on $H^1(S, \{n \text{ points}\}; \mathbb{C})$. The action of the group $\mathrm{GL}(2, \mathbb{R})$ can be seen as the action on the second term in the product

$$H^1(S, \{n \text{ points}\}; \mathbb{R} \oplus i\mathbb{R}) \simeq H^1(S, \{n \text{ points}\}; \mathbb{R}) \otimes \mathbb{R}^2 .$$

A projectivized stratum $\mathrm{P}\mathcal{H}(m_1, \dots, m_n) \simeq \mathcal{H}_1(m_1, \dots, m_n)/\mathrm{SO}(2, \mathbb{R}) \simeq \mathcal{H}(m_1, \dots, m_n)/\mathbb{C}^*$ is foliated by hyperbolic planes $\mathbb{H}^2 = \mathrm{SL}(2, \mathbb{R})/\mathrm{SO}(2, \mathbb{R})$ called *Teichmüller discs*. A natural projection of such a disc to $\mathcal{M}_g$ is an isometric immersion with respect to Teichüller metric on $\mathcal{M}_g$, so Teichmüller discs can be seen as *complex geodesics* in the Teichmüller metric on $\mathcal{M}_g$.

Similarly, any stratum of meromorphic quadratic differentials with at most simple poles is locally modeled on the anti-invariant subspace of $H^1(\hat{S}, \{n \text{ points}\}; \mathbb{C})$, where $p : \hat{S} \to S$ is the canonical double cover such that $p^*q = \omega^2$ becomes a global square of a holomorhic form ω.

Invariant measures and orbit closures

Magic Wand Theorem (A. Eskin–M. Mirzakhani–A. Mohammadi, 2014). *The closure of any $\mathrm{SL}(2,\mathbb{R})$-orbit is a suborbifold. In period coordinates any $\mathrm{GL}(2,\mathbb{R})$-orbit closure is represented by a complexification of an $\mathbb{R}$-linear subspace.*

Any ergodic $\mathrm{SL}(2,\mathbb{R})$-invariant measure is supported on a suborbifold. In period coordinates this suborbifold is represented by an affine subspace, and the invariant measure is just a usual affine measure on this affine subspace.

Theorem (S. Filip, 2014) *Any $\mathrm{GL}(2,\mathbb{R})$-invariant orbifold is, actually, an algebraic variety characterized by special arithmetic conditions.*

Theorem (A. Avila, A. Eskin. M. Möller, 2017) *Let L be a linear subspace representing a $\mathrm{GL}(2,\mathbb{R})$-orbit closure in period coordinates. The restriction of the natural symplectic form in $H^1(C,\mathbb{C})$ to the image of L under the projection $H^1(C,\{\text{zeroes}\};\mathbb{C}) \to H^1(C,\mathbb{C})$ is non-degenerate.*

“But still, my homeward way has proved too long.
While we were wasting time there, old Poseidon,
it almost seems, stretched and extended space.”

J. Brodsky

И все-таки ведущая домой
дорога оказалась слишком длинной,
как будто Посейдон, пока мы там
теряли время, растянул пространство.

И. Бродский

Idea of Renormalization

Asymptotic cycle for a torus

Consider a leaf of a measured foliation on a surface. Choose a short transversal segment X. Each time when the leaf crosses X we join the crossing point with the point x_0 along X obtaining a closed loop. Consecutive return points $x_1, x_2, \ldots$ define a sequence of cycles $c_1, c_2, \ldots$.

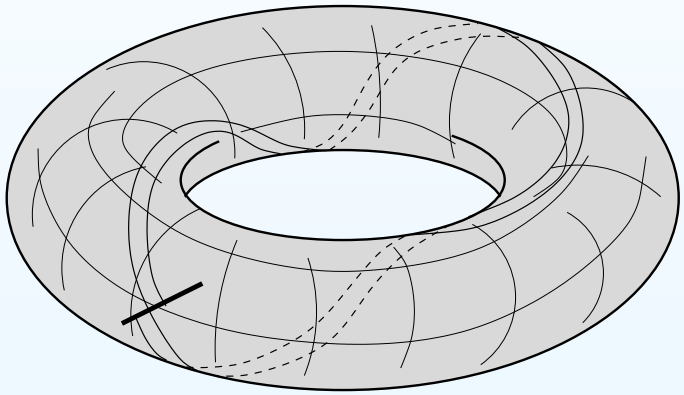

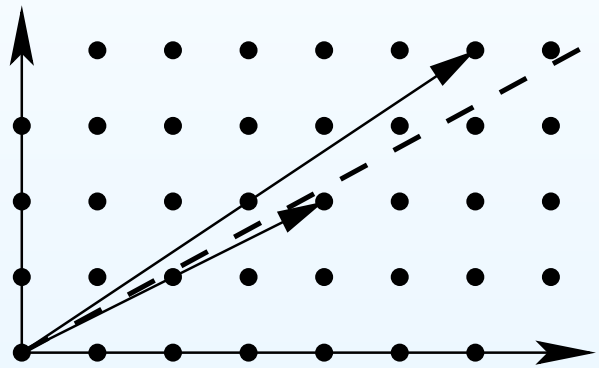

The *asymptotic cycle* is defined as $\lim_{n\to\infty} \dfrac{c_n}{n} = c \in H_1(\mathbb{T}^2; \mathbb{R})$.

Theorem (S. Kerckhoff, H. Masur, J. Smillie, 1986.) *For any flat surface directional flow in almost any direction is uniquely ergodic.*

This implies that for almost any direction the asymptotic cycle exists and is the same for all points of the surface.

Asymptotic cycle in the pseudo-Anosov case

Consider a model case of the foliation in direction of the expanding eigenvector $\vec{v}_u$ of the Anosov map $g : \mathbb{T}^2 \to \mathbb{T}^2$ with $Dg = A = \begin{pmatrix} 1 & 1 \\ 1 & 2 \end{pmatrix}$.

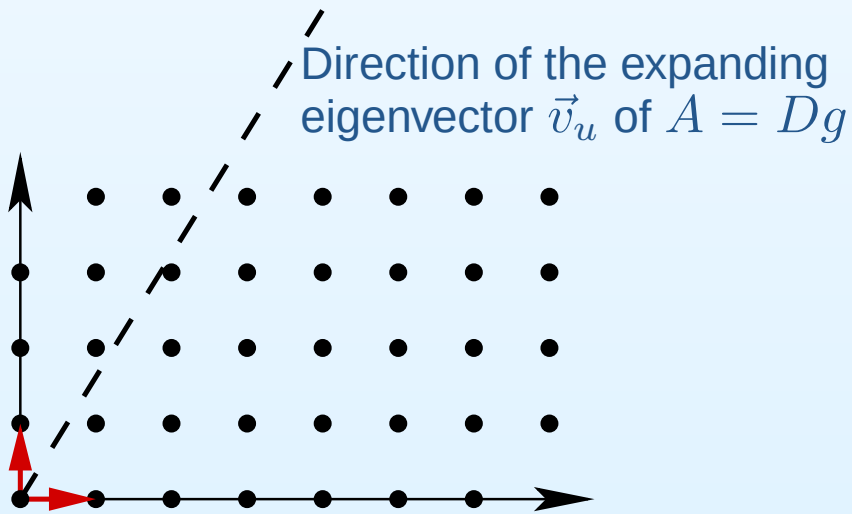

Asymptotic cycle in the pseudo-Anosov case

Consider a model case of the foliation in direction of the expanding eigenvector $\vec{v}_u$ of the Anosov map $g : \mathbb{T}^2 \to \mathbb{T}^2$ with $Dg = A = \begin{pmatrix} 1 & 1 \\ 1 & 2 \end{pmatrix}$. Take a closed curve γ and apply to it k iterations of g. The images $g_*^{(k)}(c)$ of the corresponding cycle $c = [\gamma]$ get almost collinear to the expanding eigenvector $\vec{v}_u$ of A, and the corresponding curve $g^{(k)}(\gamma)$ closely follows our foliation.

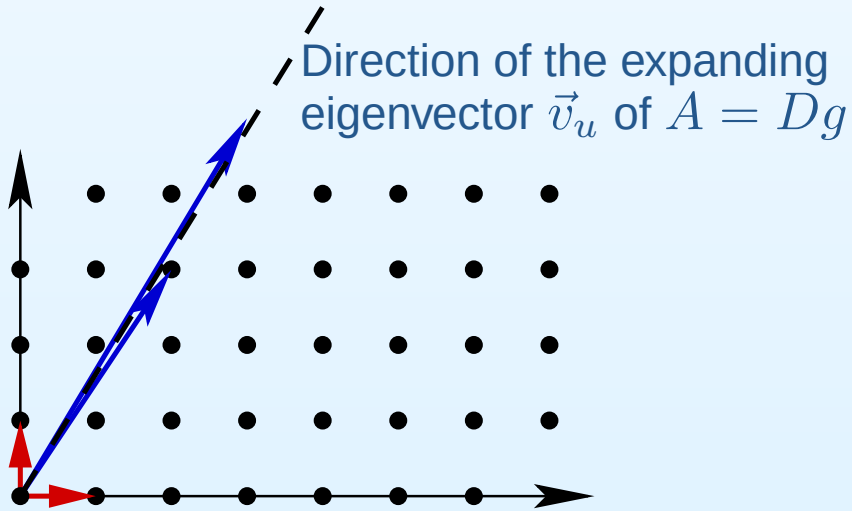

Asymptotic cycle in the pseudo-Anosov case

Consider a model case of the foliation in direction of the expanding eigenvector $\vec{v}_u$ of the Anosov map $g : \mathbb{T}^2 \to \mathbb{T}^2$ with $Dg = A = \begin{pmatrix} 1 & 1 \\ 1 & 2 \end{pmatrix}$. Take a closed curve γ and apply to it k iterations of g. The images $g_*^{(k)}(c)$ of the corresponding cycle $c = [\gamma]$ get almost collinear to the expanding eigenvector $\vec{v}_u$ of A, and the corresponding curve $g^{(k)}(\gamma)$ closely follows our foliation.

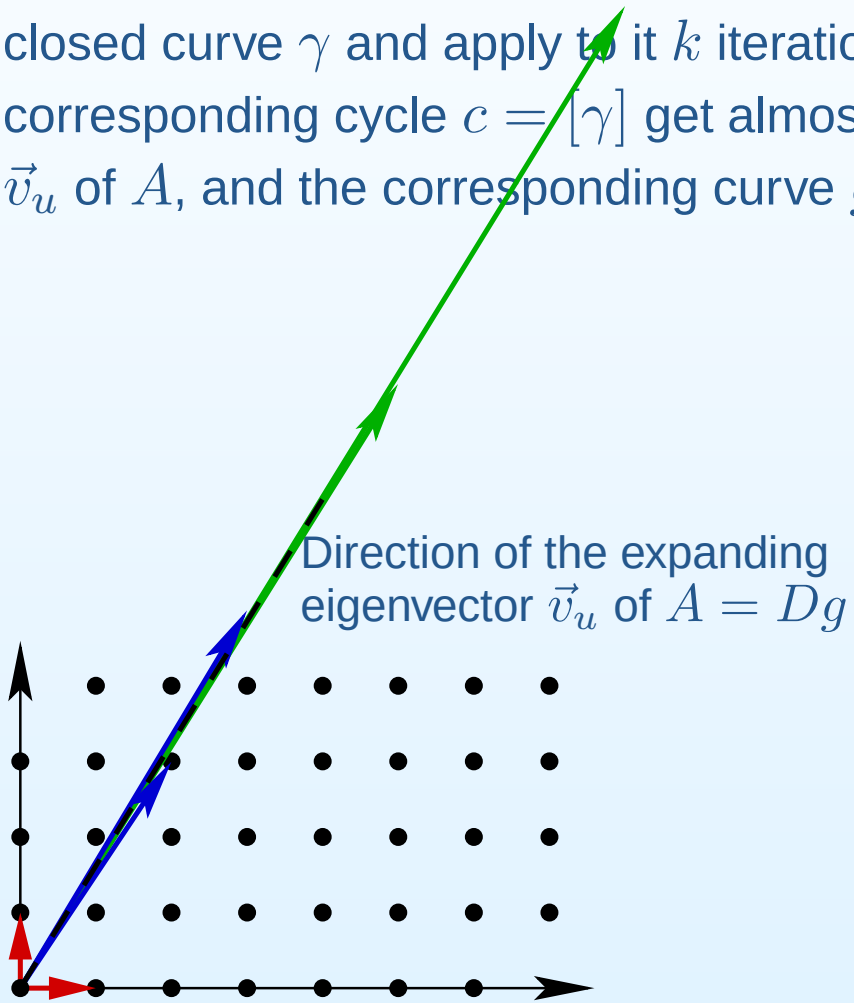

Asymptotic cycle in the pseudo-Anosov case

Consider a model case of the foliation in direction of the expanding eigenvector $\vec{v}_u$ of the Anosov map $g : \mathbb{T}^2 \to \mathbb{T}^2$ with $Dg = A = \begin{pmatrix} 1 & 1 \\ 1 & 2 \end{pmatrix}$. Take a closed curve γ and apply to it k iterations of g. The images $g_*^{(k)}(c)$ of the corresponding cycle $c = [\gamma]$ get almost collinear to the expanding eigenvector $\vec{v}_u$ of A, and the corresponding curve $g^{(k)}(\gamma)$ closely follows our foliation.

The first return cycles to a short subinterval exhibit exactly the same behavior by a simple reason that they are images of the first return cycles to a longer subinterval under a high iteration of g.

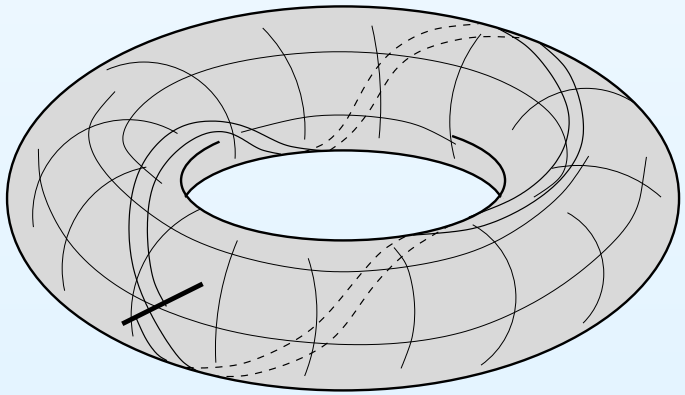

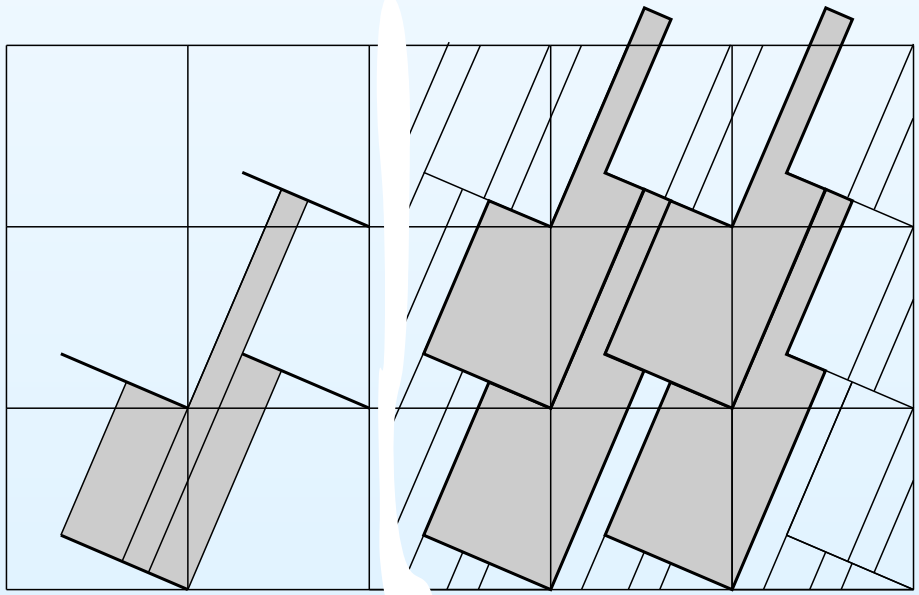

Zippered rectangles

For a general flat surface S the first return map of the vertical flow to a horizontal segment X also induces an interval exchange transformation $T : X \to X$.

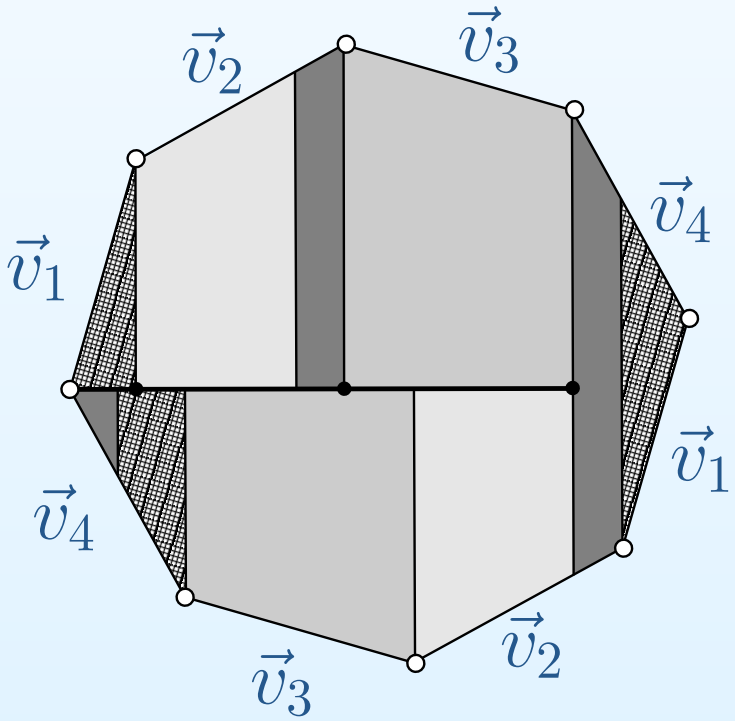

Zippered rectangles

We get a decomposition of S into *zippered rectangles*.

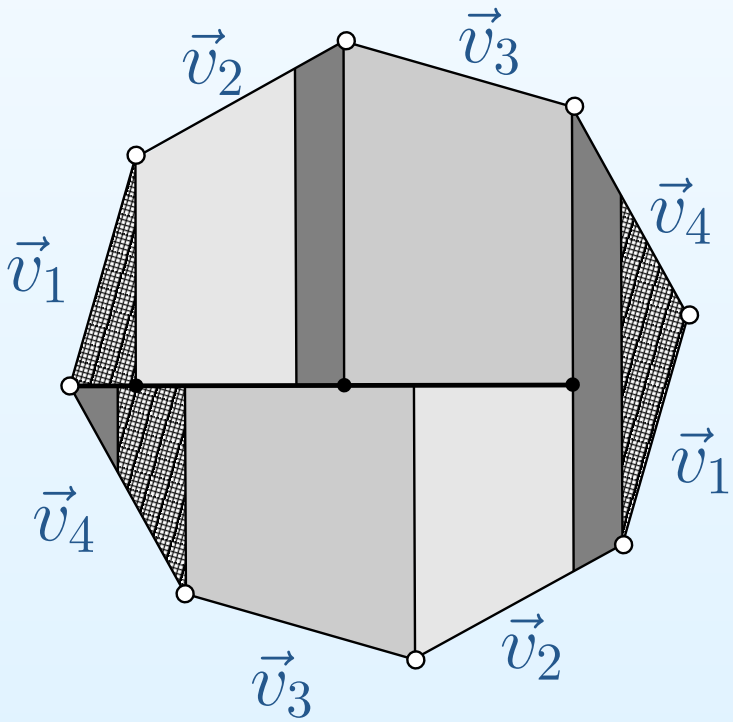

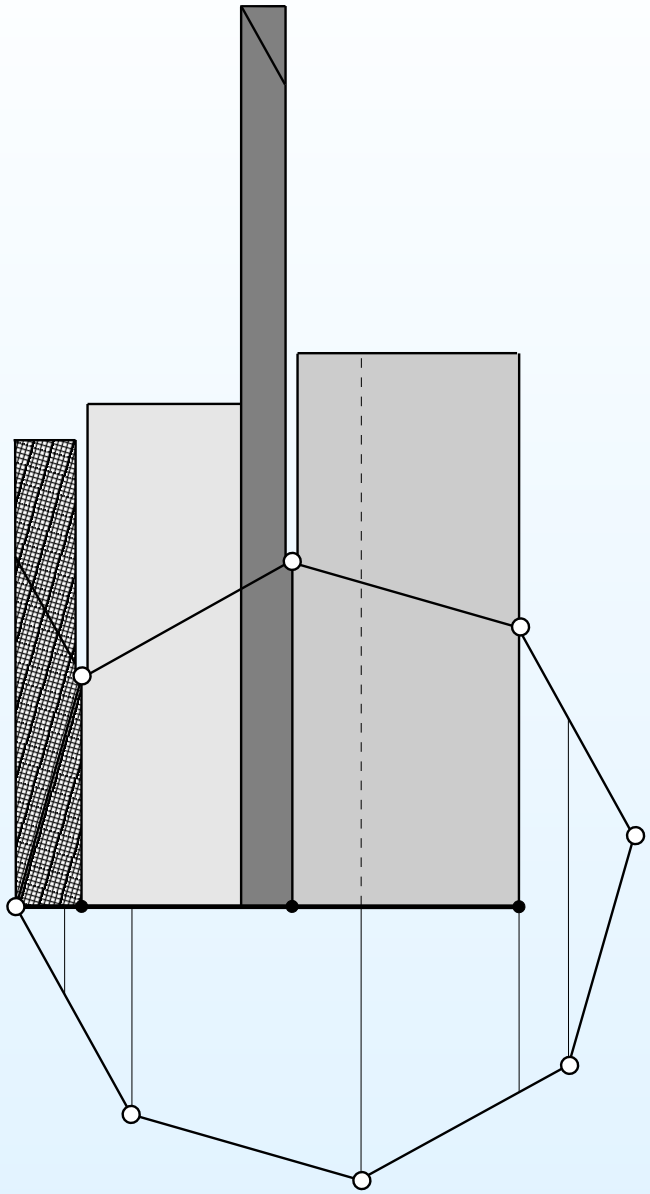

First return cycles

Launch the vertical trajectory from a point $x \in X$. When the trajectory intersects X for the first time join the corresponding point $T(x)$ to the original point x along X to obtain a closed loop $c(x)$. (In the picture this “first return cycle” is smoothed.)

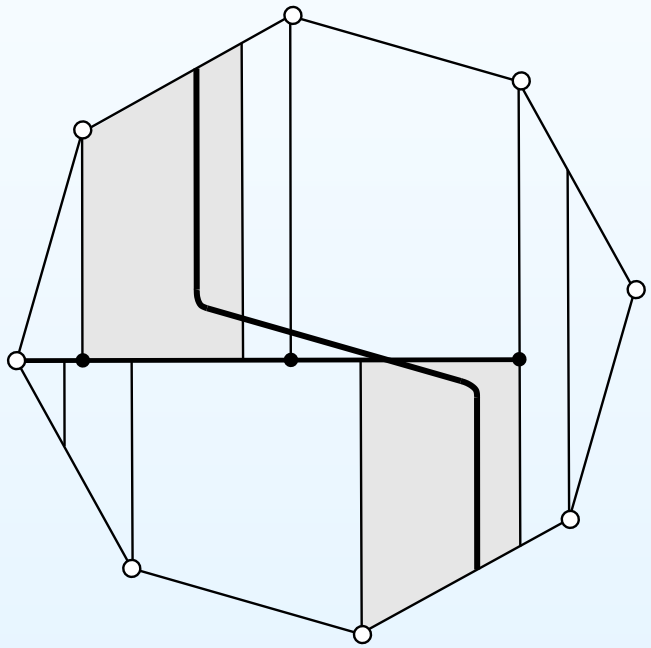

First return cycles

Launch the vertical trajectory from a point $x \in X$. When the trajectory intersects X for the first time join the corresponding point $T(x)$ to the original point x along X to obtain a closed loop $c(x)$. (In the picture this "first return cycle" is smoothed.)

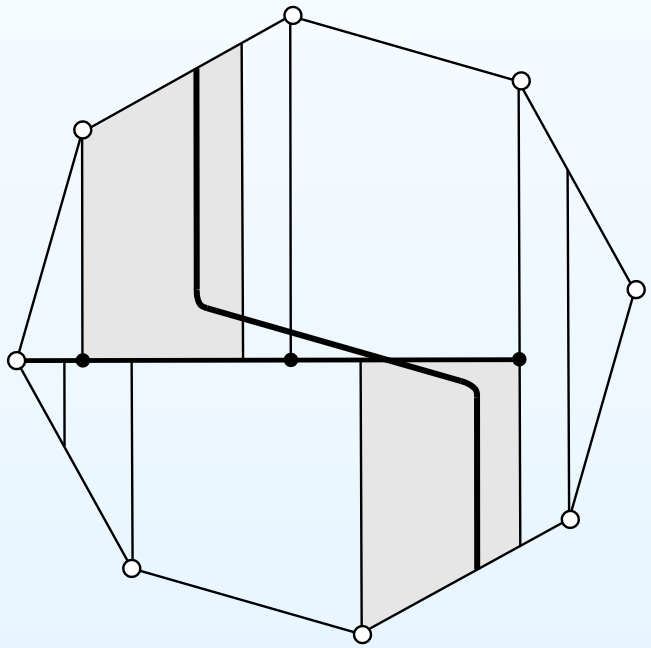

The cycle $c_N(x)$ obtained after N returns of the vertical trajectory to X can be computed as:

$$c_N(x) = c(x) + c(T(x)) + \cdots + c(T^{N-1}(x))$$

First return cycles

The “first return cycle” $c(x)$ is constant
on every subinterval X_j; denote it by $c(X_j)$.

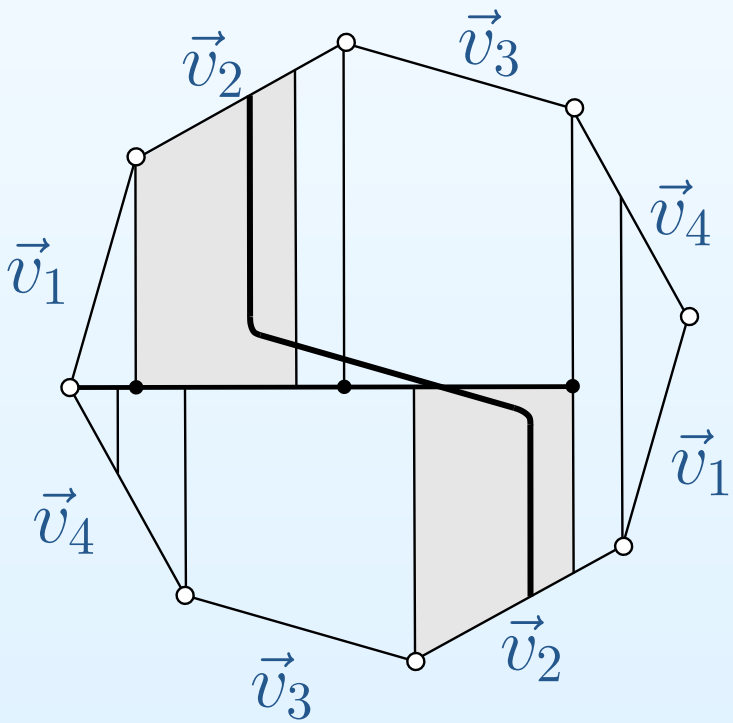

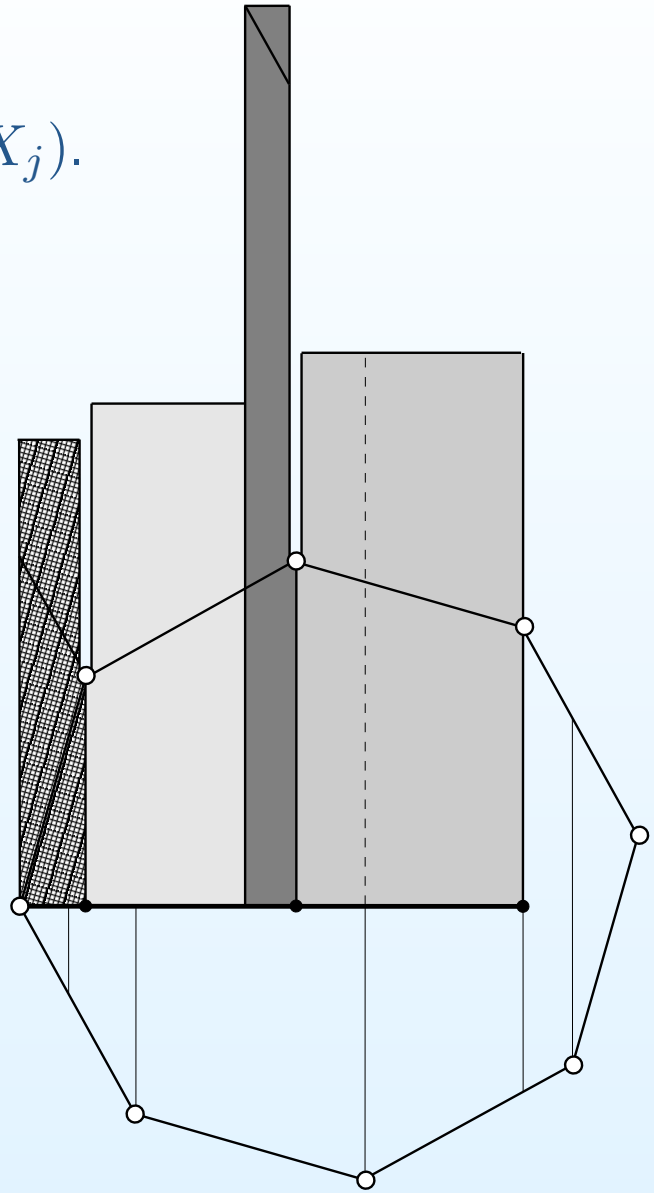

One step of renormalization

Consider a subinterval $X' \subset X$. Choose it in such way that that the first return map to X' induces an interval exchange transformation $T' : X' \to X'$ of the same number n of subintervals.

New first return cycles $c'(X'_k)$ to the interval X' are expressed in terms of the initial first return cycles $c(X_j)$ by linear relations; the lengths $|X'_k|$ of subintervals of the new partition $X' = X'_1 \sqcup \cdots \sqcup X'_n$ are expressed in terms of the lengths $|X_j|$ of subintervals of the initial partition by dual linear relations:

$$c'(X'_k) = \sum_{j=1}^{n} A_{jk} \cdot c(X_j) \qquad\qquad |X_j| = \sum_{k=1}^{n} A_{jk} \cdot |X'_k| \,,$$

Here a nonnegative integer matrix A_{jk} is completely determined by the initial interval exchange transformation $T : X \to X$ and by the choice of $X' \subset X$.

Idea of renormalization

Unwrap the flat surface into “zippered rectangles”. Shorten the base.

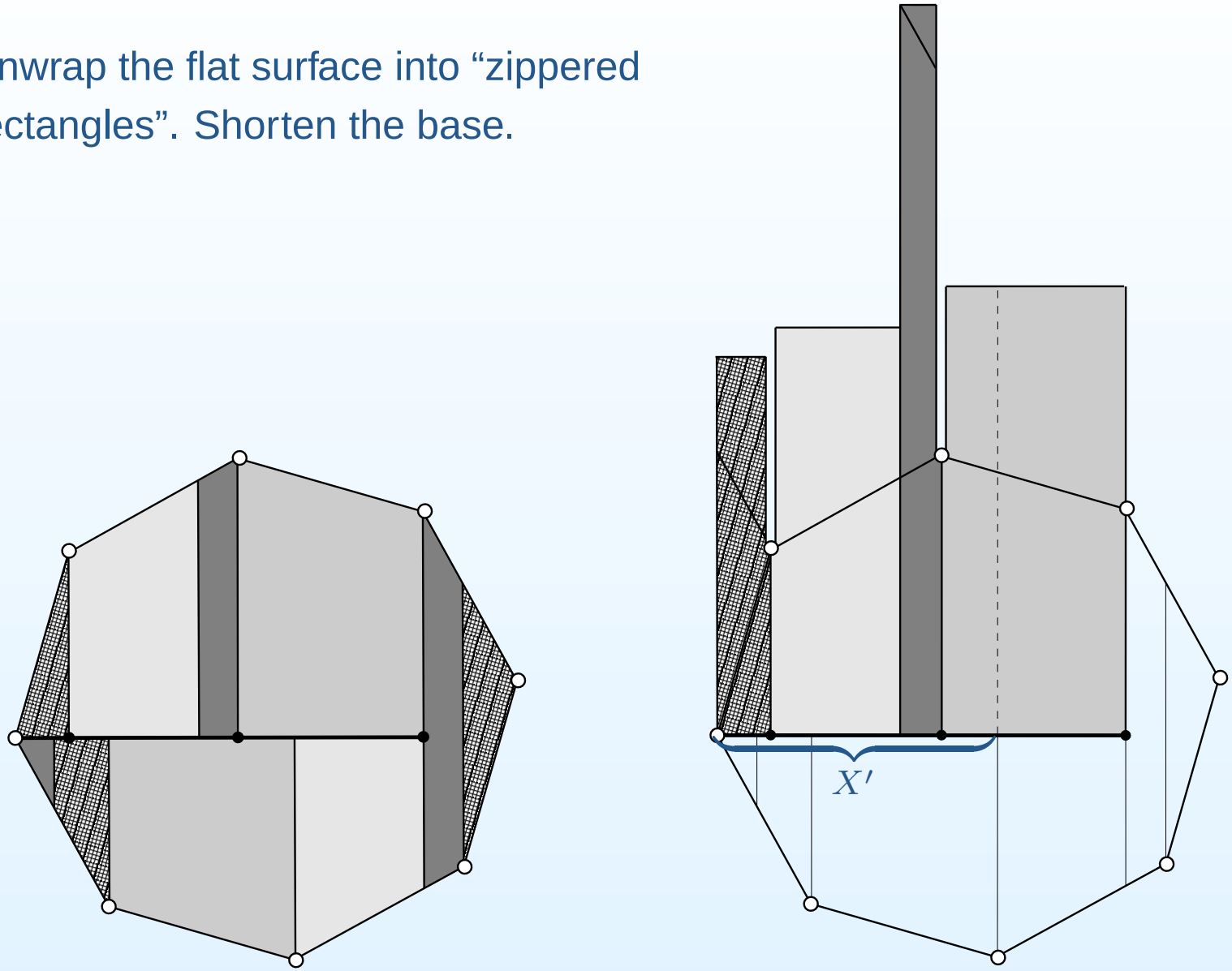

Idea of a renormalization

Expand the resulting tall and narrow zippered rectangles horizontally and contract them vertically by a factor e^{t_0}.

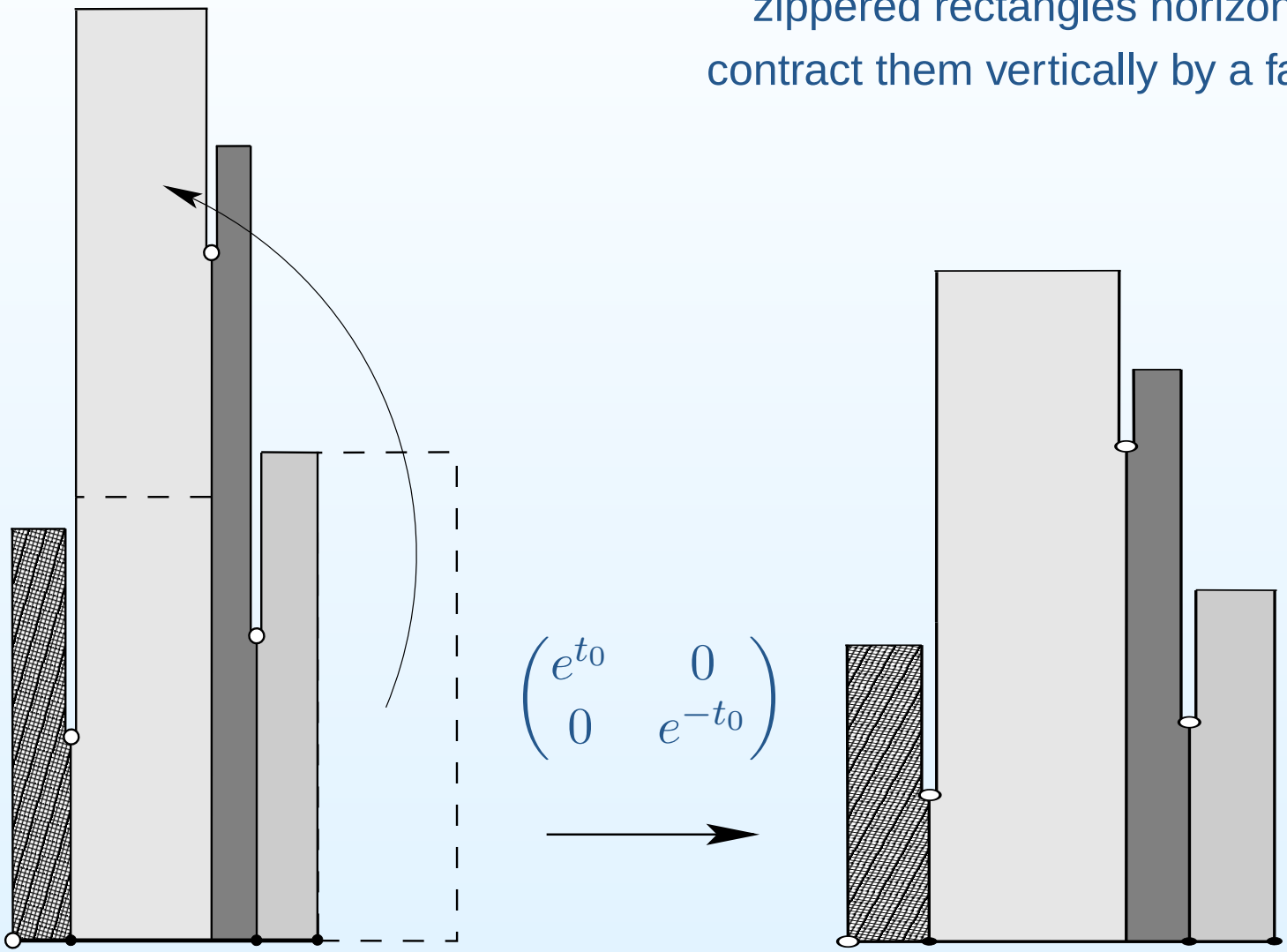

Idea of a renormalization

Lemma (Veech). *If a translation surface S admits a pseudo-Anosov diffeomorphism $f = g_{t_0}$ contracting the vertical and expanding the horizontal directions, (i.e. if $g_{t_0}(S) = S$ for some t_0), then we will detect it (possibly as a power f^k) in our discrete procedure of shortening the base X. The corresponding matrix A_{jk} represents the induced map $f^k_* : H_1(S;\mathbb{Z}) \to H_1(S;\mathbb{Z})$.*

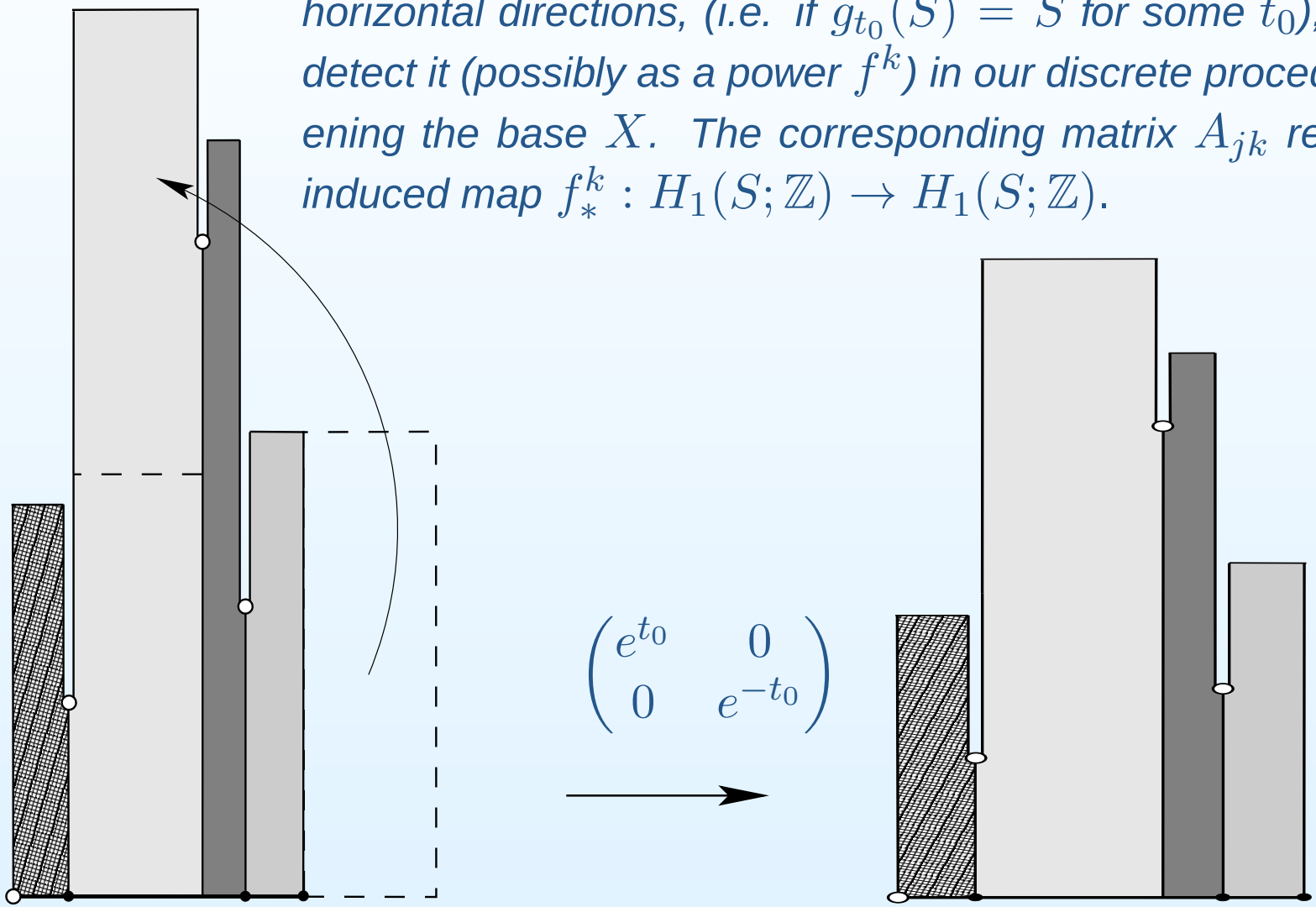

Idea of a renormalization

By the theorem of Masur and Veech, the homogeneous expansion-contraction in vertical-horizontal directions regularly brings almost any flat surface, basically, back to itself. *Multiplicative ergodic theorem* states that, in a sense, there a matrix (one and the same for almost all flat surfaces) which mimics a matrix of a “universal” pseudo-Anosov diffeomorphism as if the Teichmüller flow would be periodic.

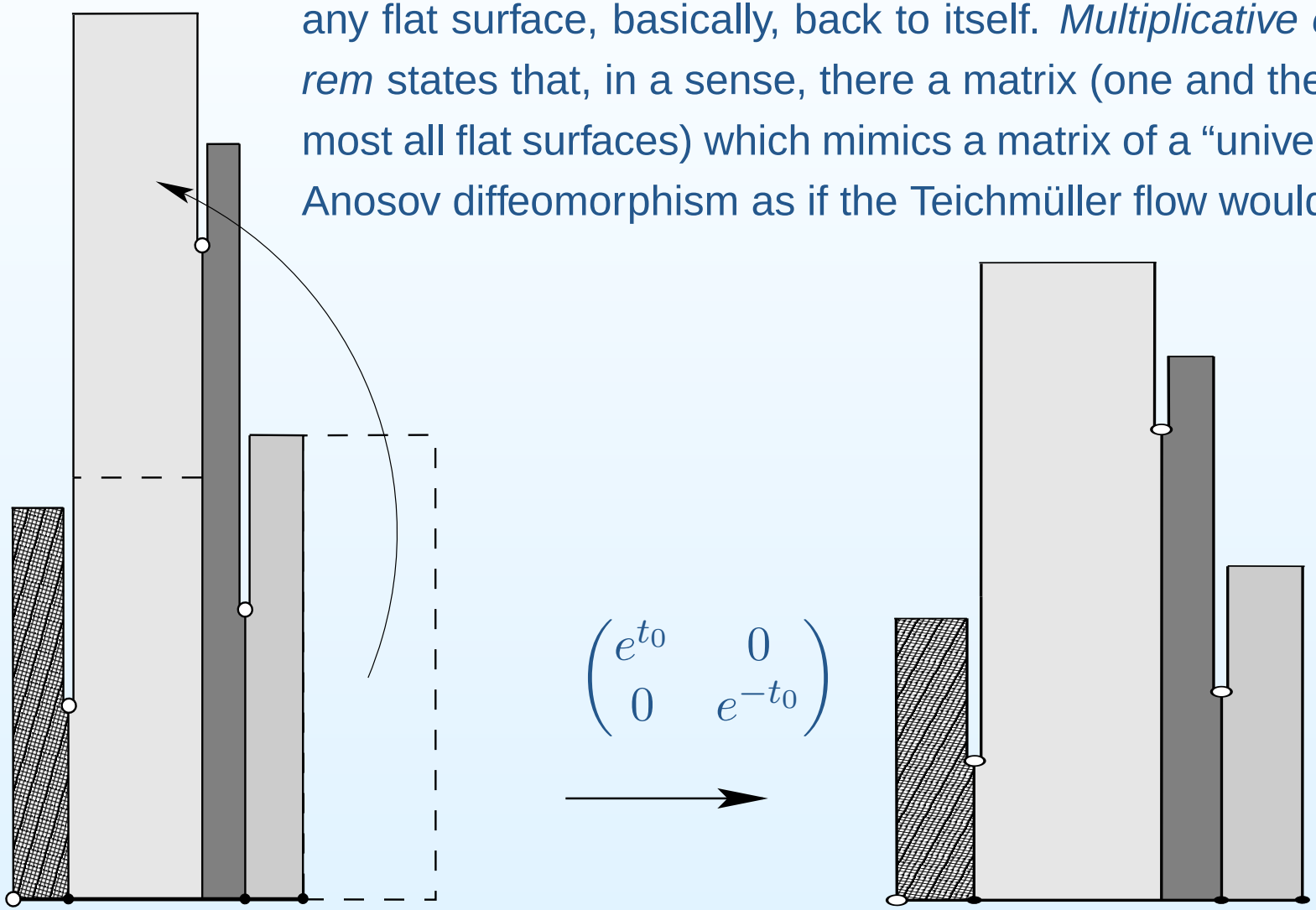

Time acceleration machine

To construct the cycle c_N representing a long piece of trajectory of the vertical flow we follow the trajectory $x, T(x), \dots, T^{N-1}(x)$ of the corresponding interval exchange transformation and compute the corresponding ergodic sum $c_N(x) = c(x) + \cdots + c(T^{N-1}(x))$.

Passing to a subinterval $X' \subset X$ we can follow the trajectory $x, T'(x), \dots, (T')^{N'-1}(x)$ of the new interval exchange transformation $T' : X' \to X'$. Since X' is shorter than X we cover the initial piece of trajectory of the vertical flow in a smaller number N' of steps.

Passing from T to T' we accelerate the time: that the trajectory $x, T'(x), \dots, (T')^{N'-1}(x)$ follows the trajectory $x, T(x), \dots, T^{N-1}(x)$ but jumps over several iterations of T at a time.

Our renormalization consists in considering first return cycles to a special shorter subinterval. Formally, it can be seen as a map on the space of interval exchange transformations, combined with rescaling the interval to keep unit length. Applying several iterations of the renormalization map we obtain exponentially long trajectory of the initial first return map.

Spectrum of “mean monodromy”

Consider a vector bundle endowed with a flat connection over a manifold X^n. Having a flow on the base we can take a fiber of the vector bundle and transport it along a trajectory of the flow. When the trajectory comes close to the starting point we identify the fibers using the connection and we get a linear transformation $\mathcal{A}(x,1)$ of the fiber; the next time we get a matrix $\mathcal{A}(x,2)$, etc.

The multiplicative ergodic theorem says that when the flow is ergodic a *“matrix of mean monodromy”* along the flow

$$A_{mean} := \lim_{N\to\infty} (\mathcal{A}^*(x,N)\cdot\mathcal{A}(x,N))^{\frac{1}{2N}}$$

is well-defined and constant for almost every starting point.

Lyapunov exponents correspond to logarithms of eigenvalues of this “matrix of mean monodromy”. They measure the average growth rate of the norm of vectors of the bundle when we pull them along the flow using the connection. Lyapunov exponents are dynamical analogs of characteristic numbers of the bundle. It is known that they are responsible for the diffusion rate.

Spectrum of “mean monodromy”

Consider a vector bundle endowed with a flat connection over a manifold X^n. Having a flow on the base we can take a fiber of the vector bundle and transport it along a trajectory of the flow. When the trajectory comes close to the starting point we identify the fibers using the connection and we get a linear transformation $\mathcal{A}(x,1)$ of the fiber; the next time we get a matrix $\mathcal{A}(x,2)$, etc.

The multiplicative ergodic theorem says that when the flow is ergodic a *“matrix of mean monodromy”* along the flow

$$A_{mean} := \lim_{N\to\infty} (\mathcal{A}^*(x,N)\cdot\mathcal{A}(x,N))^{\frac{1}{2N}}$$

is well-defined and constant for almost every starting point.

Lyapunov exponents correspond to logarithms of eigenvalues of this “matrix of mean monodromy”. They measure the average growth rate of the norm of vectors of the bundle when we pull them along the flow using the connection. Lyapunov exponents are dynamical analogs of characteristic numbers of the bundle. It is known that they are responsible for the diffusion rate.

Gauss–Manin connection

Diffeomorphisms of surfaces

Observation 1. *Surfaces can wrap around themselves.*

Cut a torus along a horizontal circle.

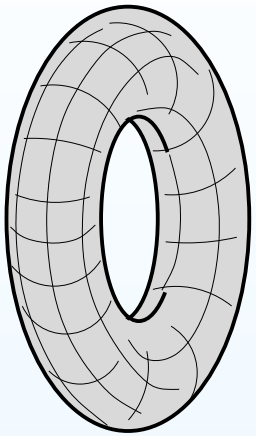

Diffeomorphisms of surfaces

Observation 1. *Surfaces can wrap around themselves.*

Dehn twist twists progressively horizontal circles up to a complete turn on the opposite boundary component of the cylinder and then identifies the components.

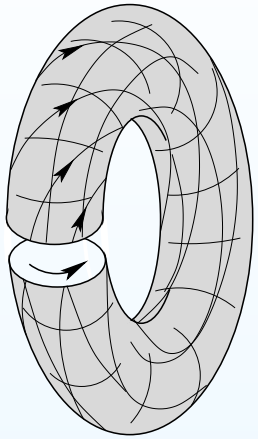

Diffeomorphisms of surfaces

Observation 1. *Surfaces can wrap around themselves.*

Dehn twist twists progressively horizontal circles up to a complete turn on the opposite boundary component of the cylinder and then identifies the components.

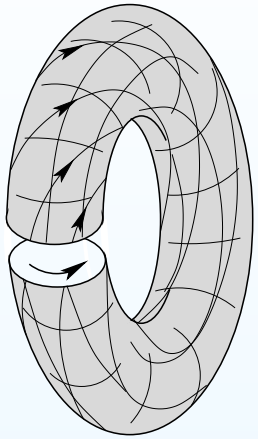

$$\begin{array}{ccc} \mathbb{R}^2 & \xrightarrow{\hat{f}_h} & \mathbb{R}^2 \\ \downarrow & & \downarrow \\ \mathbb{R}^2/\mathbb{Z}^2 = \mathbb{T}^2 & \xrightarrow[f_h]{} & \mathbb{T}^2 = \mathbb{R}^2/\mathbb{Z}^2 \end{array}$$

Dehn twist corresponds to the linear map $\hat{f}_h : \mathbb{R}^2 \to \mathbb{R}^2$ with the matrix $\begin{pmatrix} 1 & 1 \\ 0 & 1 \end{pmatrix}$.

Diffeomorphisms of surfaces

Observation 1. *Surfaces can wrap around themselves.*

Dehn twist twists progressively horizontal circles up to a complete turn on the opposite boundary component of the cylinder and then identifies the components.

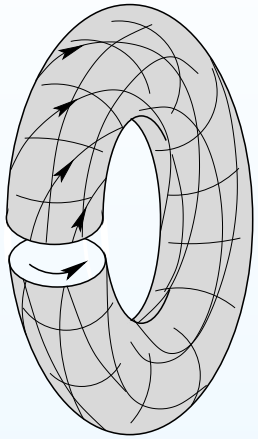

$$\begin{array}{ccc} \mathbb{R}^2 & \xrightarrow{\hat{f}_h} & \mathbb{R}^2 \\ \downarrow & & \downarrow \\ \mathbb{R}^2/\mathbb{Z}^2 = \mathbb{T}^2 & \xrightarrow[f_h]{} & \mathbb{T}^2 = \mathbb{R}^2/\mathbb{Z}^2 \end{array}$$

Dehn twist corresponds to the linear map $\hat{f}_h : \mathbb{R}^2 \to \mathbb{R}^2$ with the matrix $\begin{pmatrix} 1 & 1 \\ 0 & 1 \end{pmatrix}$.

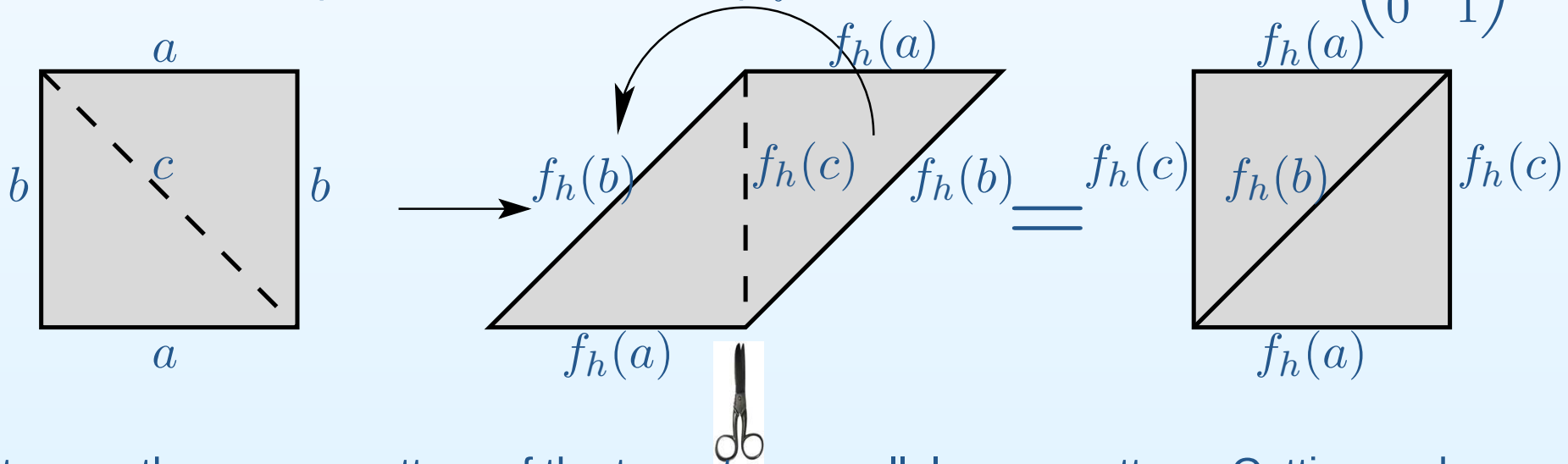

It maps the square pattern of the torus to a parallelogram pattern. Cutting and pasting appropriately we can transform the new pattern to the initial square.

Diffeomorphisms of surfaces

Observation 1. *Surfaces can wrap around themselves.*

Dehn twist twists progressively horizontal circles up to a complete turn on the opposite boundary component of the cylinder and then identifies the components.

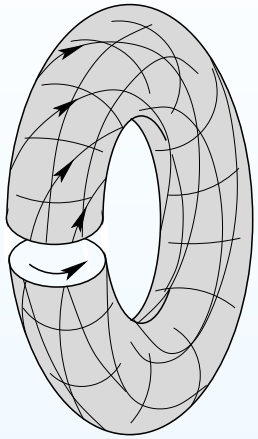

$$\begin{array}{ccc} \mathbb{R}^2 & \xrightarrow{\hat{f}_h} & \mathbb{R}^2 \\ \downarrow & & \downarrow \\ \mathbb{R}^2/\mathbb{Z}^2 = \mathbb{T}^2 & \xrightarrow[f_h]{} & \mathbb{T}^2 = \mathbb{R}^2/\mathbb{Z}^2 \end{array}$$

Dehn twist corresponds to the linear map $\hat{f}_h : \mathbb{R}^2 \to \mathbb{R}^2$ with the matrix $\begin{pmatrix} 1 & 1 \\ 0 & 1 \end{pmatrix}$.

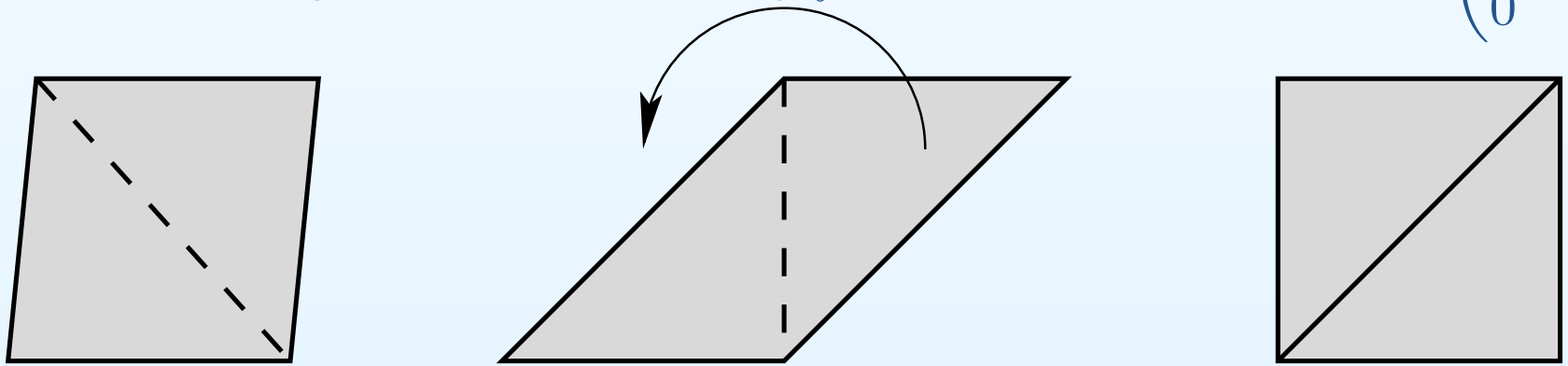

Changing the slope of the parallelogram pattern progressively we get a *closed path* in the space of flat tori.

Diffeomorphisms of surfaces

Observation 1. *Surfaces can wrap around themselves.*

Dehn twist twists progressively horizontal circles up to a complete turn on the opposite boundary component of the cylinder and then identifies the components.

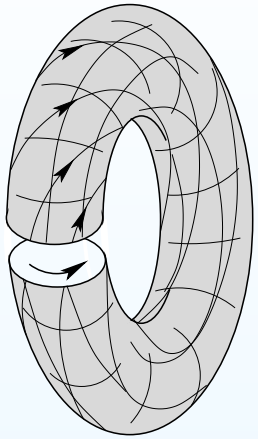

$$\begin{array}{ccc} \mathbb{R}^2 & \xrightarrow{\hat{f}_h} & \mathbb{R}^2 \\ \downarrow & & \downarrow \\ \mathbb{R}^2/\mathbb{Z}^2 = \mathbb{T}^2 & \xrightarrow[f_h]{} & \mathbb{T}^2 = \mathbb{R}^2/\mathbb{Z}^2 \end{array}$$

Dehn twist corresponds to the linear map $\hat{f}_h : \mathbb{R}^2 \to \mathbb{R}^2$ with the matrix $\begin{pmatrix} 1 & 1 \\ 0 & 1 \end{pmatrix}$.

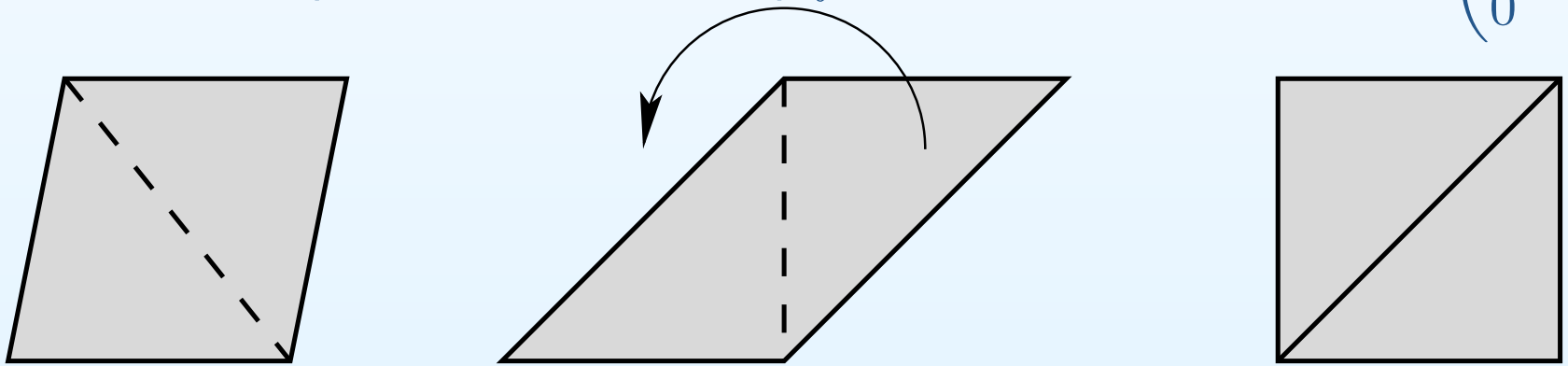

Changing the slope of the parallelogram pattern progressively we get a *closed path* in the space of flat tori.

Diffeomorphisms of surfaces

Observation 1. *Surfaces can wrap around themselves.*

Dehn twist twists progressively horizontal circles up to a complete turn on the opposite boundary component of the cylinder and then identifies the components.

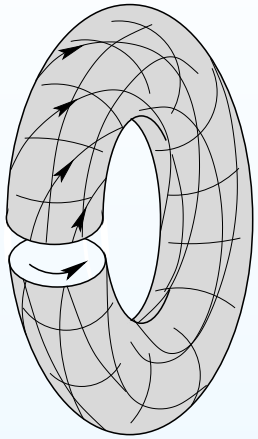

$$\begin{array}{ccc} \mathbb{R}^2 & \xrightarrow{\hat{f}_h} & \mathbb{R}^2 \\ \downarrow & & \downarrow \\ \mathbb{R}^2/\mathbb{Z}^2 = \mathbb{T}^2 & \xrightarrow[f_h]{} & \mathbb{T}^2 = \mathbb{R}^2/\mathbb{Z}^2 \end{array}$$

Dehn twist corresponds to the linear map $\hat{f}_h : \mathbb{R}^2 \to \mathbb{R}^2$ with the matrix $\begin{pmatrix} 1 & 1 \\ 0 & 1 \end{pmatrix}$.

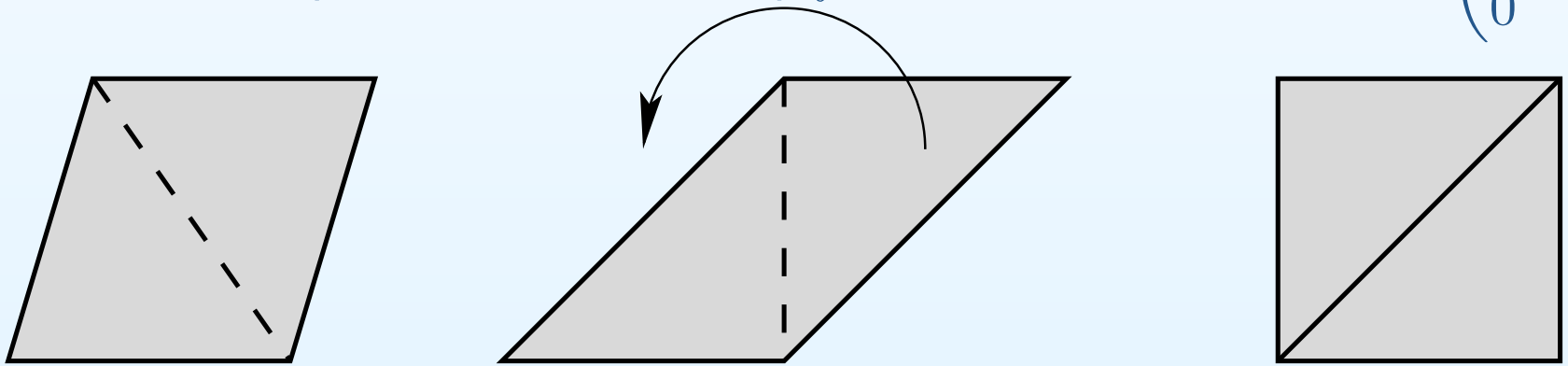

Changing the slope of the parallelogram pattern progressively we get a *closed path* in the space of flat tori.

Diffeomorphisms of surfaces

Observation 1. *Surfaces can wrap around themselves.*

Dehn twist twists progressively horizontal circles up to a complete turn on the opposite boundary component of the cylinder and then identifies the components.

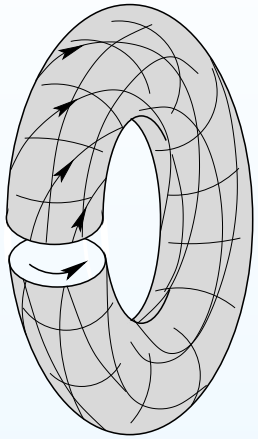

$$\begin{array}{ccc} \mathbb{R}^2 & \xrightarrow{\hat{f}_h} & \mathbb{R}^2 \\ \downarrow & & \downarrow \\ \mathbb{R}^2/\mathbb{Z}^2 = \mathbb{T}^2 & \xrightarrow[f_h]{} & \mathbb{T}^2 = \mathbb{R}^2/\mathbb{Z}^2 \end{array}$$

Dehn twist corresponds to the linear map $\hat{f}_h : \mathbb{R}^2 \to \mathbb{R}^2$ with the matrix $\begin{pmatrix} 1 & 1 \\ 0 & 1 \end{pmatrix}$.

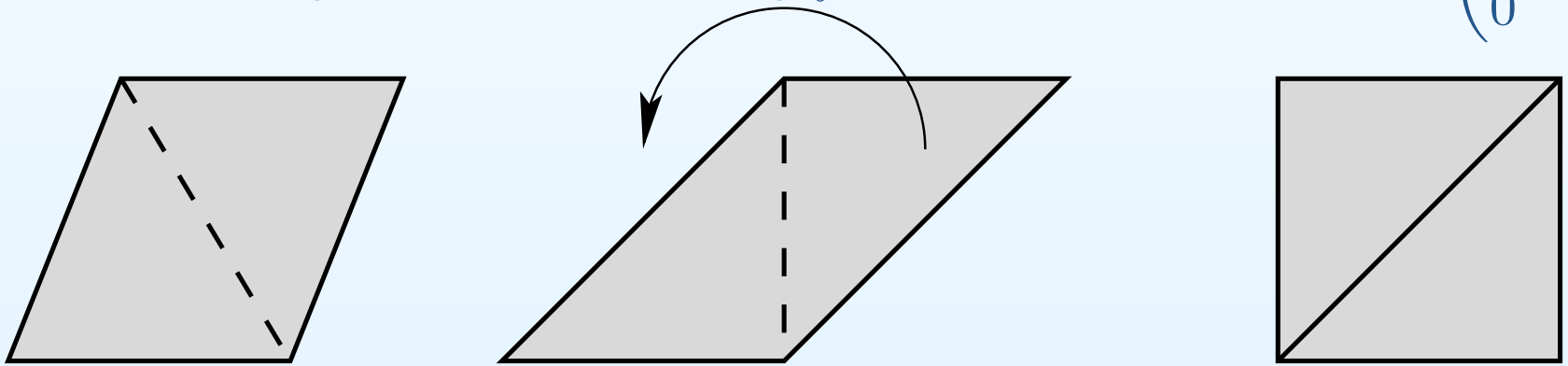

Changing the slope of the parallelogram pattern progressively we get a *closed path* in the space of flat tori.

Diffeomorphisms of surfaces

Observation 1. *Surfaces can wrap around themselves.*

Dehn twist twists progressively horizontal circles up to a complete turn on the opposite boundary component of the cylinder and then identifies the components.

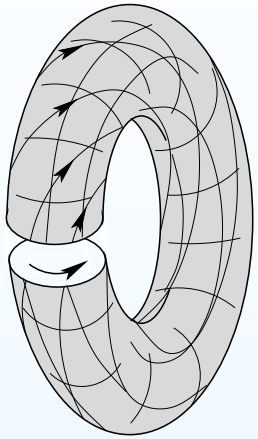

$$\begin{array}{ccc} \mathbb{R}^2 & \xrightarrow{\hat{f}_h} & \mathbb{R}^2 \\ \downarrow & & \downarrow \\ \mathbb{R}^2/\mathbb{Z}^2 = \mathbb{T}^2 & \xrightarrow[f_h]{} & \mathbb{T}^2 = \mathbb{R}^2/\mathbb{Z}^2 \end{array}$$

Dehn twist corresponds to the linear map $\hat{f}_h : \mathbb{R}^2 \to \mathbb{R}^2$ with the matrix $\begin{pmatrix} 1 & 1 \\ 0 & 1 \end{pmatrix}$.

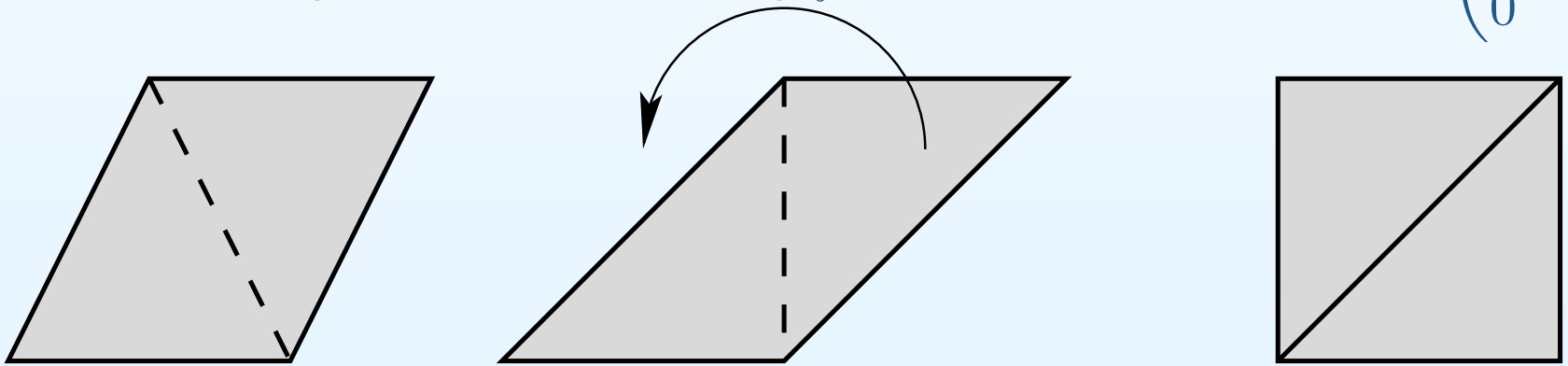

Changing the slope of the parallelogram pattern progressively we get a *closed path* in the space of flat tori.

Diffeomorphisms of surfaces

Observation 1. *Surfaces can wrap around themselves.*

Dehn twist twists progressively horizontal circles up to a complete turn on the opposite boundary component of the cylinder and then identifies the components.

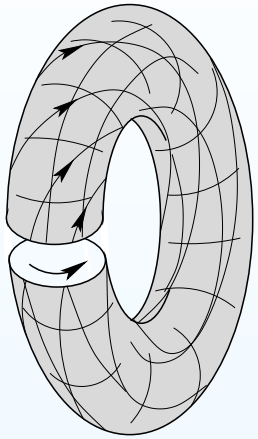

$$\begin{array}{ccc} \mathbb{R}^2 & \xrightarrow{\hat{f}_h} & \mathbb{R}^2 \\ \downarrow & & \downarrow \\ \mathbb{R}^2/\mathbb{Z}^2 = \mathbb{T}^2 & \xrightarrow[f_h]{} & \mathbb{T}^2 = \mathbb{R}^2/\mathbb{Z}^2 \end{array}$$

Dehn twist corresponds to the linear map $\hat{f}_h : \mathbb{R}^2 \to \mathbb{R}^2$ with the matrix $\begin{pmatrix} 1 & 1 \\ 0 & 1 \end{pmatrix}$.

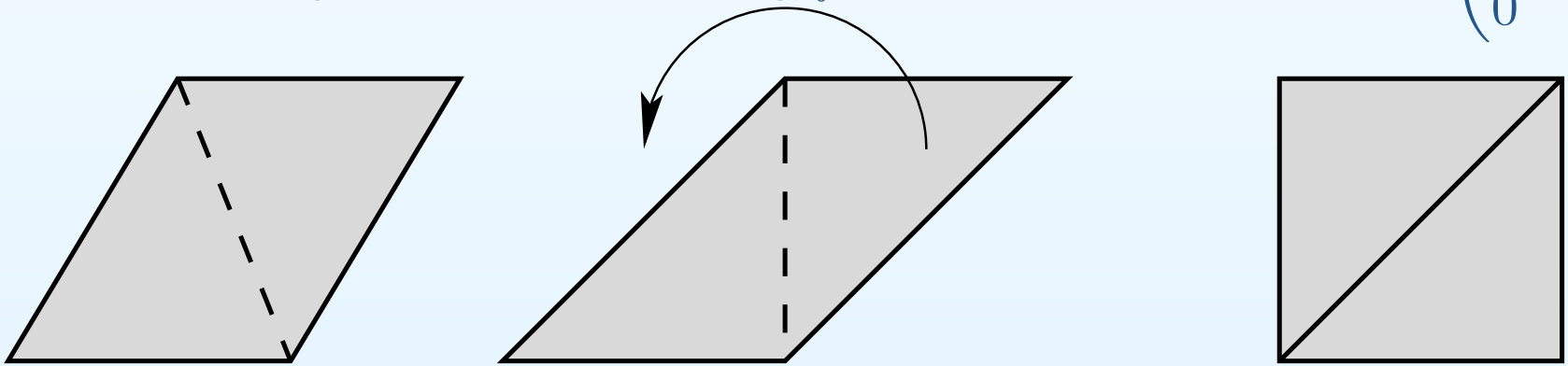

Changing the slope of the parallelogram pattern progressively we get a *closed path* in the space of flat tori.

Diffeomorphisms of surfaces

Observation 1. *Surfaces can wrap around themselves.*

Dehn twist twists progressively horizontal circles up to a complete turn on the opposite boundary component of the cylinder and then identifies the components.

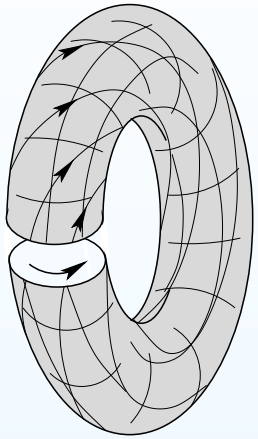

$$\begin{array}{ccc} \mathbb{R}^2 & \xrightarrow{\hat{f}_h} & \mathbb{R}^2 \\ \downarrow & & \downarrow \\ \mathbb{R}^2/\mathbb{Z}^2 = \mathbb{T}^2 & \xrightarrow[f_h]{} & \mathbb{T}^2 = \mathbb{R}^2/\mathbb{Z}^2 \end{array}$$

Dehn twist corresponds to the linear map $\hat{f}_h : \mathbb{R}^2 \to \mathbb{R}^2$ with the matrix $\begin{pmatrix} 1 & 1 \\ 0 & 1 \end{pmatrix}$.

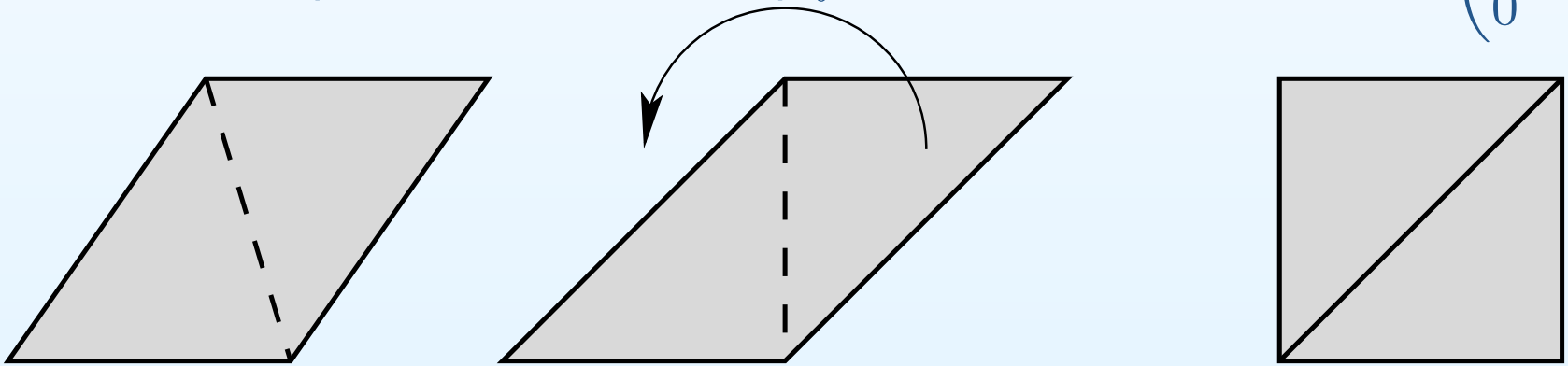

Changing the slope of the parallelogram pattern progressively we get a *closed path* in the space of flat tori.

Diffeomorphisms of surfaces

Observation 1. *Surfaces can wrap around themselves.*

Dehn twist twists progressively horizontal circles up to a complete turn on the opposite boundary component of the cylinder and then identifies the components.

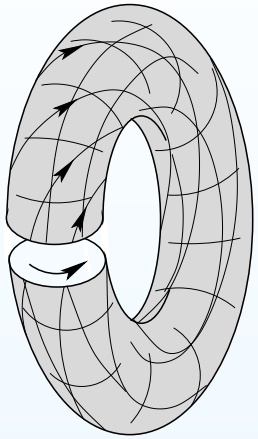

$$\begin{array}{ccc} \mathbb{R}^2 & \xrightarrow{\hat{f}_h} & \mathbb{R}^2 \\ \downarrow & & \downarrow \\ \mathbb{R}^2/\mathbb{Z}^2 = \mathbb{T}^2 & \xrightarrow[f_h]{} & \mathbb{T}^2 = \mathbb{R}^2/\mathbb{Z}^2 \end{array}$$

Dehn twist corresponds to the linear map $\hat{f}_h : \mathbb{R}^2 \to \mathbb{R}^2$ with the matrix $\begin{pmatrix} 1 & 1 \\ 0 & 1 \end{pmatrix}$.

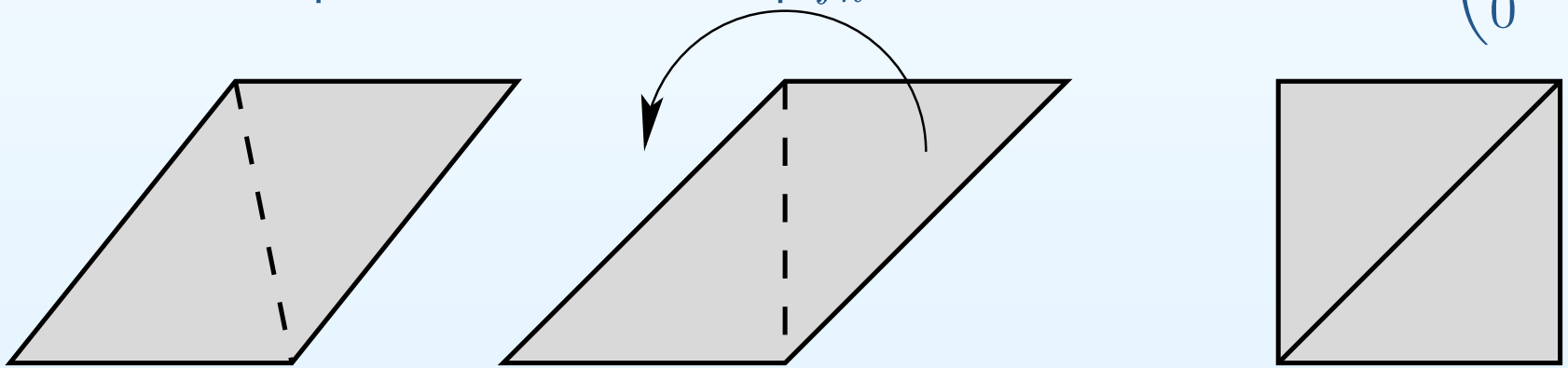

Changing the slope of the parallelogram pattern progressively we get a *closed path* in the space of flat tori.

Diffeomorphisms of surfaces

Observation 1. *Surfaces can wrap around themselves.*

Dehn twist twists progressively horizontal circles up to a complete turn on the opposite boundary component of the cylinder and then identifies the components.

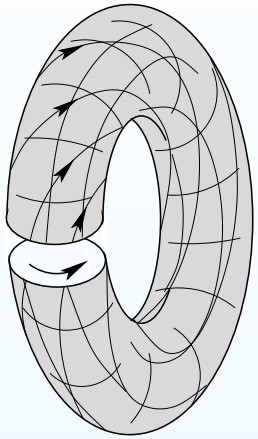

$$\begin{array}{ccc} \mathbb{R}^2 & \xrightarrow{\hat{f}_h} & \mathbb{R}^2 \\ \downarrow & & \downarrow \\ \mathbb{R}^2/\mathbb{Z}^2 = \mathbb{T}^2 & \xrightarrow[f_h]{} & \mathbb{T}^2 = \mathbb{R}^2/\mathbb{Z}^2 \end{array}$$

Dehn twist corresponds to the linear map $\hat{f}_h : \mathbb{R}^2 \to \mathbb{R}^2$ with the matrix $\begin{pmatrix} 1 & 1 \\ 0 & 1 \end{pmatrix}$.

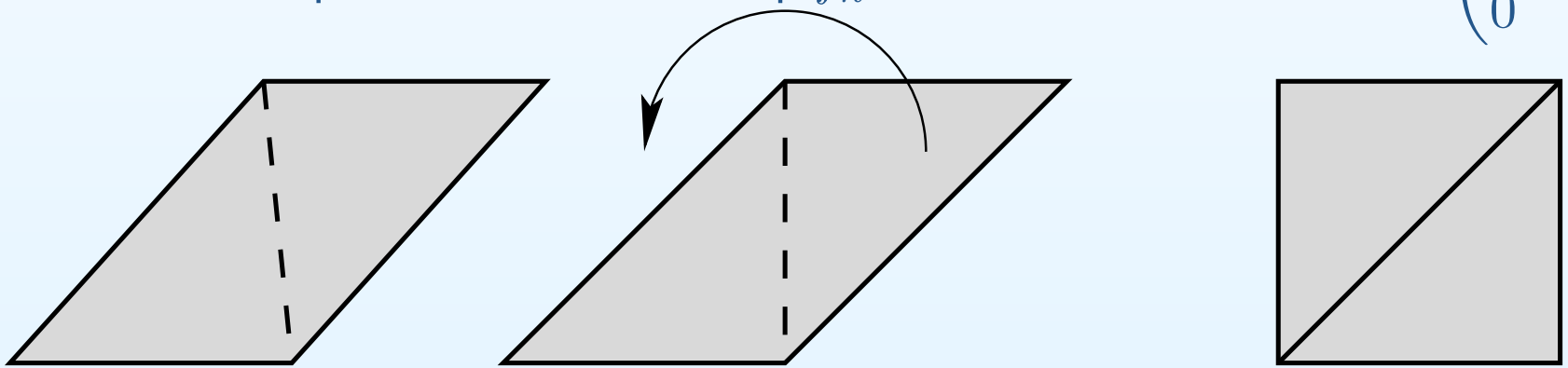

Changing the slope of the parallelogram pattern progressively we get a *closed path* in the space of flat tori.

Diffeomorphisms of surfaces

Observation 1. *Surfaces can wrap around themselves.*

Dehn twist twists progressively horizontal circles up to a complete turn on the opposite boundary component of the cylinder and then identifies the components.

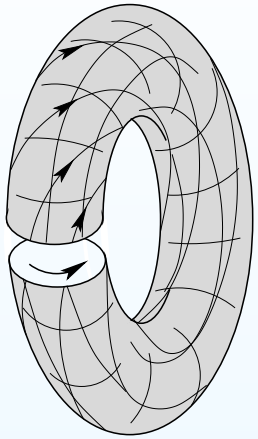

$$\begin{array}{ccc} \mathbb{R}^2 & \xrightarrow{\hat{f}_h} & \mathbb{R}^2 \\ \downarrow & & \downarrow \\ \mathbb{R}^2/\mathbb{Z}^2 = \mathbb{T}^2 & \xrightarrow[f_h]{} & \mathbb{T}^2 = \mathbb{R}^2/\mathbb{Z}^2 \end{array}$$

Dehn twist corresponds to the linear map $\hat{f}_h : \mathbb{R}^2 \to \mathbb{R}^2$ with the matrix $\begin{pmatrix} 1 & 1 \\ 0 & 1 \end{pmatrix}$.

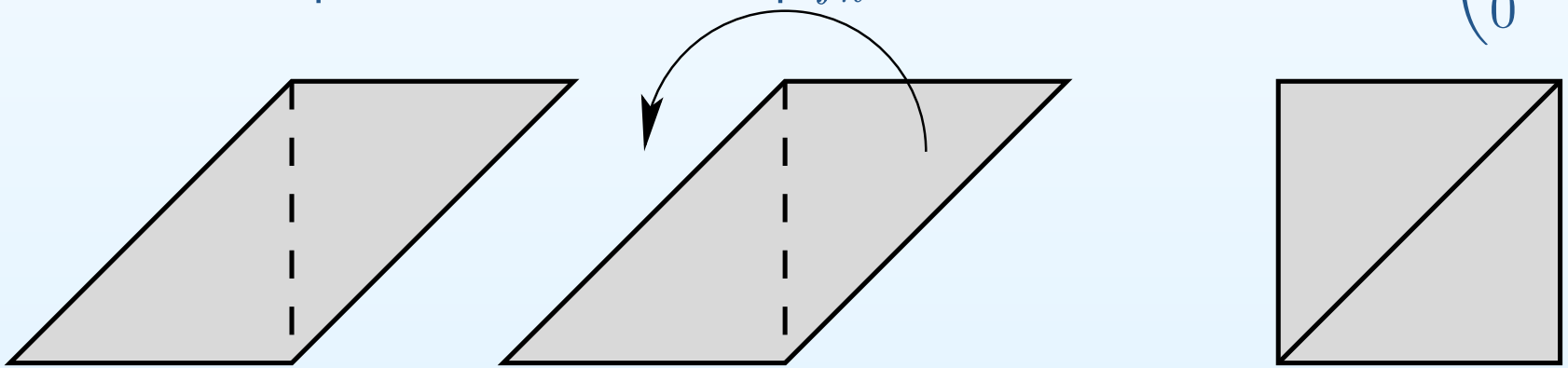

Changing the slope of the parallelogram pattern progressively we get a *closed path* in the space of flat tori.

Diffeomorphisms of surfaces

Observation 1. *Surfaces can wrap around themselves.*

Dehn twist twists progressively horizontal circles up to a complete turn on the opposite boundary component of the cylinder and then identifies the components.

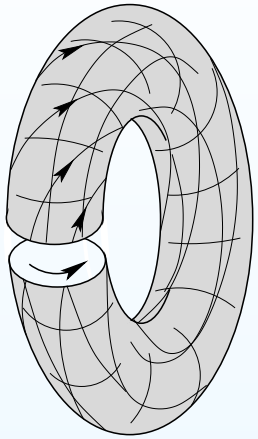

$$\begin{array}{ccc} \mathbb{R}^2 & \xrightarrow{\hat{f}_h} & \mathbb{R}^2 \\ \downarrow & & \downarrow \\ \mathbb{R}^2/\mathbb{Z}^2 = \mathbb{T}^2 & \xrightarrow[f_h]{} & \mathbb{T}^2 = \mathbb{R}^2/\mathbb{Z}^2 \end{array}$$

Dehn twist corresponds to the linear map $\hat{f}_h : \mathbb{R}^2 \to \mathbb{R}^2$ with the matrix $\begin{pmatrix} 1 & 1 \\ 0 & 1 \end{pmatrix}$.

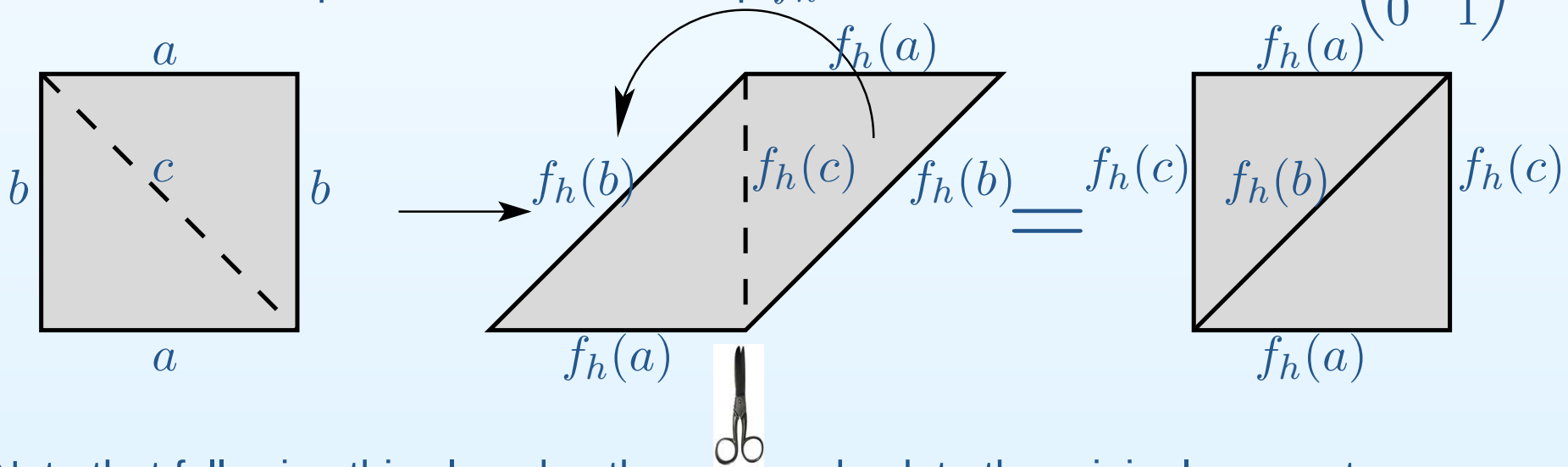

Note that following this closed path we come back to the original square torus having twisted the homology!

Closed horocycle in the moduli space of tori

Projection of a similar closed orbit of the *horocyclic flow* $\begin{pmatrix} 1 & t \\ 0 & 1 \end{pmatrix}$ to the moduli space of flat tori.

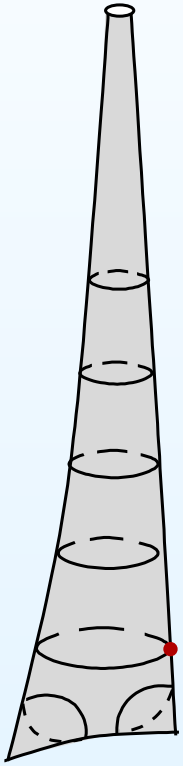

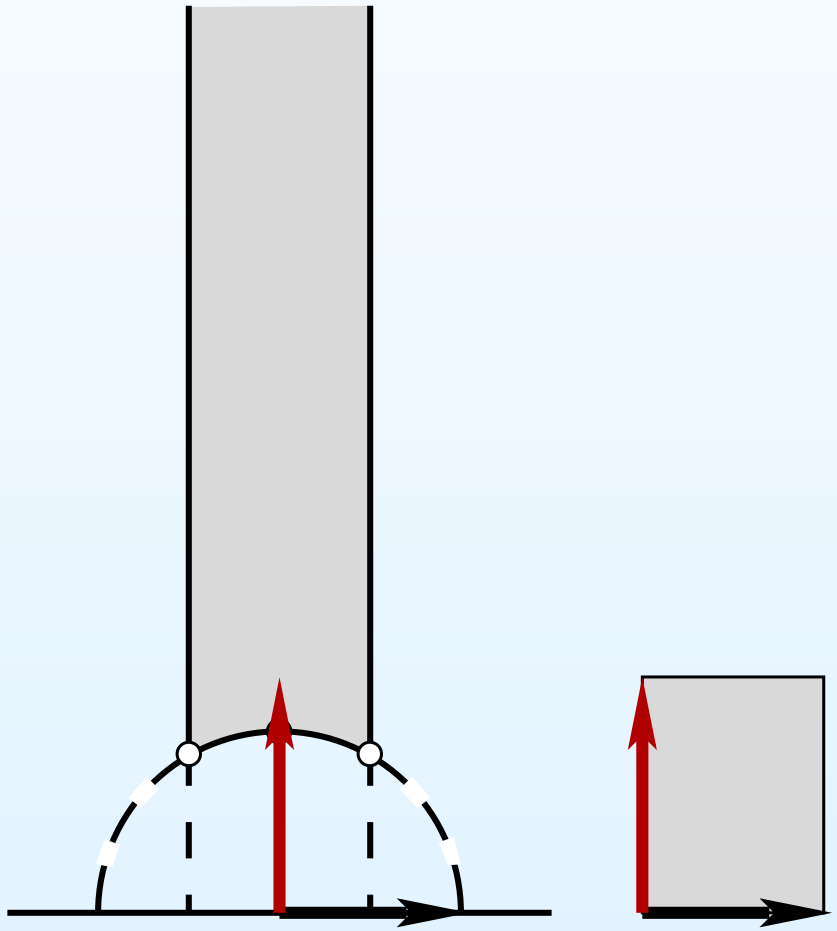

Closed horocycle in the moduli space of tori

Projection of a similar closed orbit of the *horocyclic flow* $\begin{pmatrix} 1 & t \\ 0 & 1 \end{pmatrix}$ to the moduli space of flat tori.

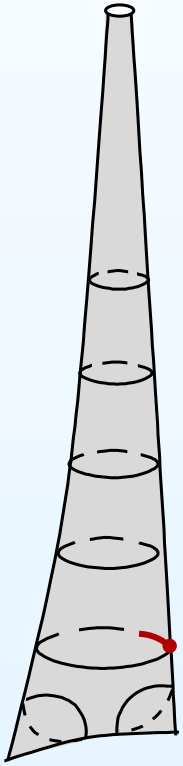

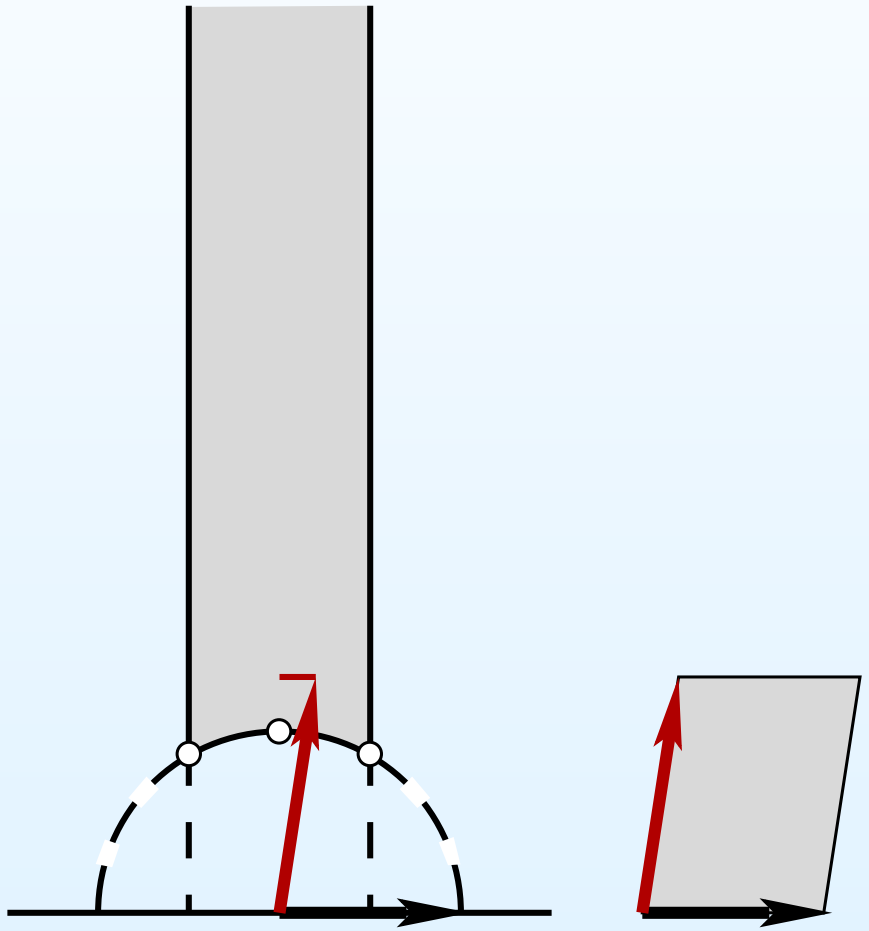

Closed horocycle in the moduli space of tori

Projection of a similar closed orbit of the *horocyclic flow* $\begin{pmatrix} 1 & t \\ 0 & 1 \end{pmatrix}$ to the moduli space of flat tori.

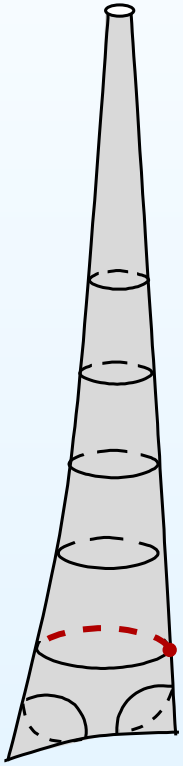

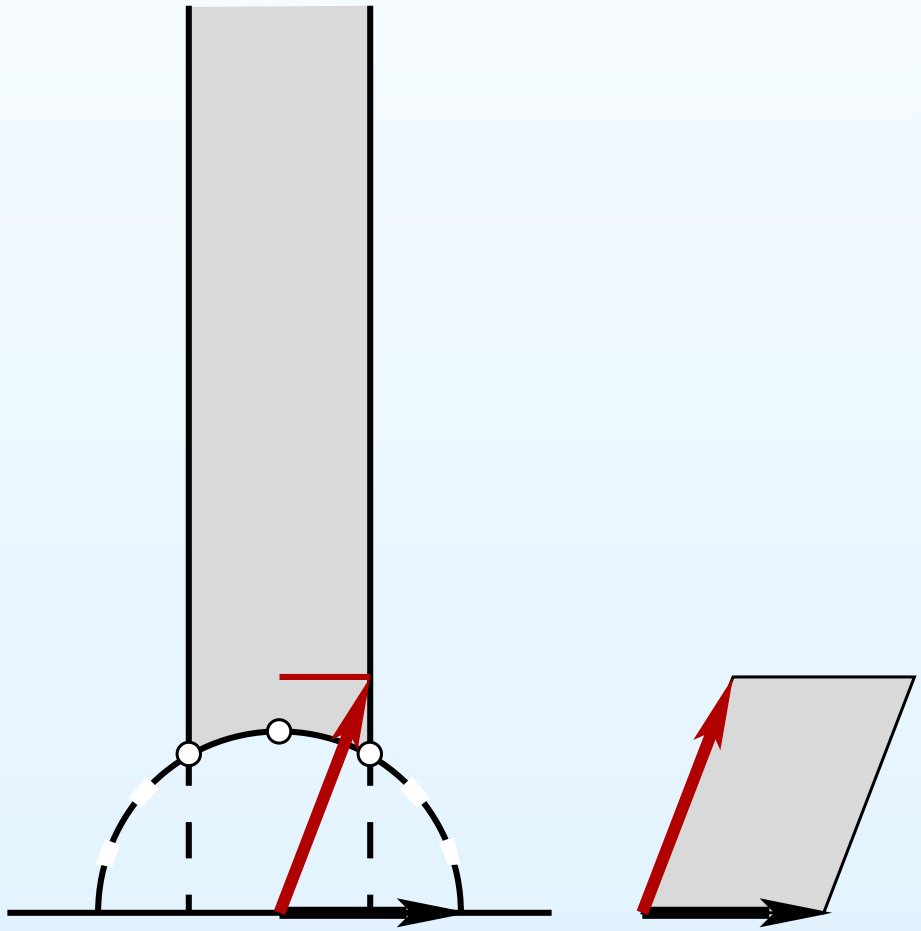

Closed horocycle in the moduli space of tori

Projection of a similar closed orbit of the *horocyclic flow* $\begin{pmatrix} 1 & t \\ 0 & 1 \end{pmatrix}$ to the moduli space of flat tori.

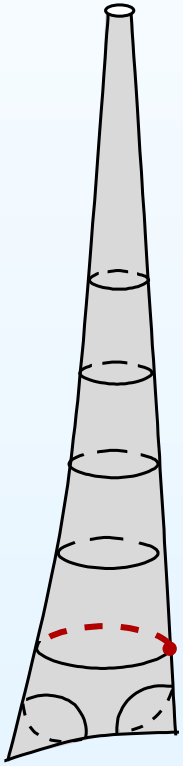

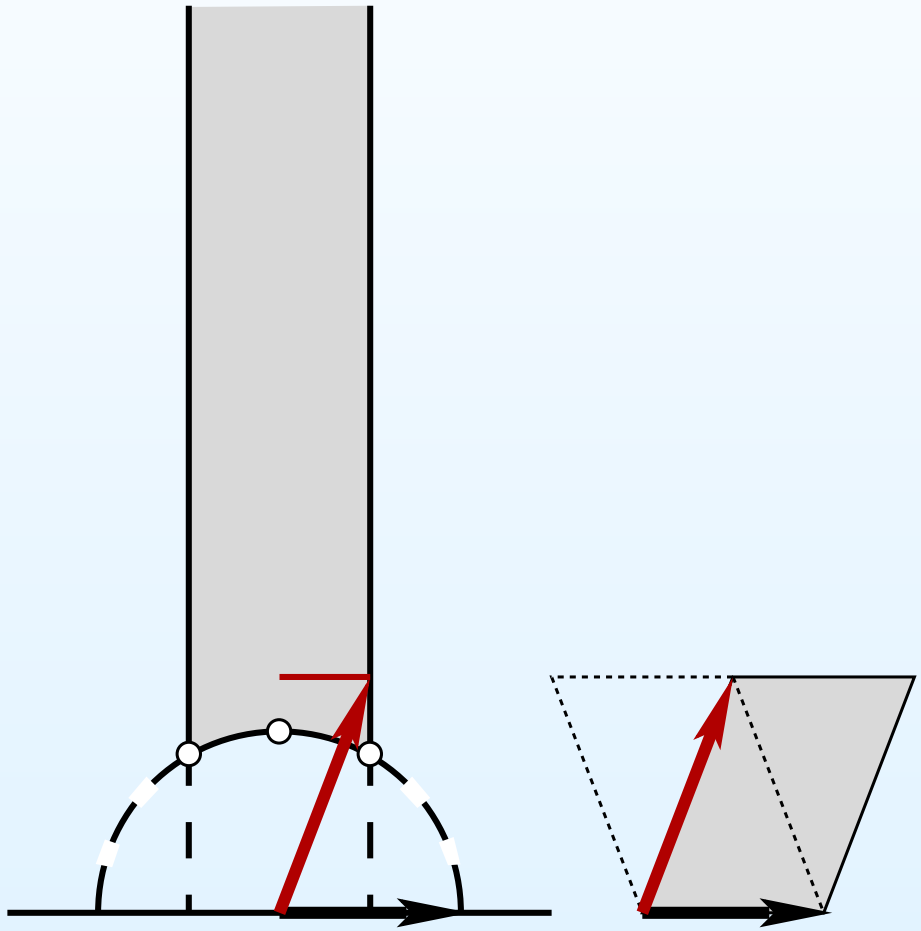

Closed horocycle in the moduli space of tori

Projection of a similar closed orbit of the *horocyclic flow* $\begin{pmatrix} 1 & t \\ 0 & 1 \end{pmatrix}$ to the moduli space of flat tori.

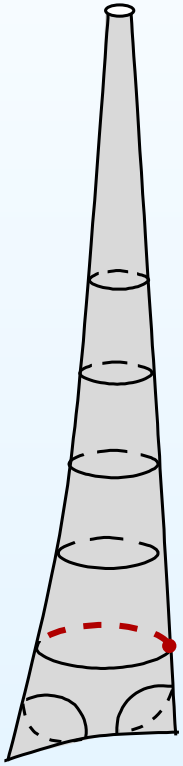

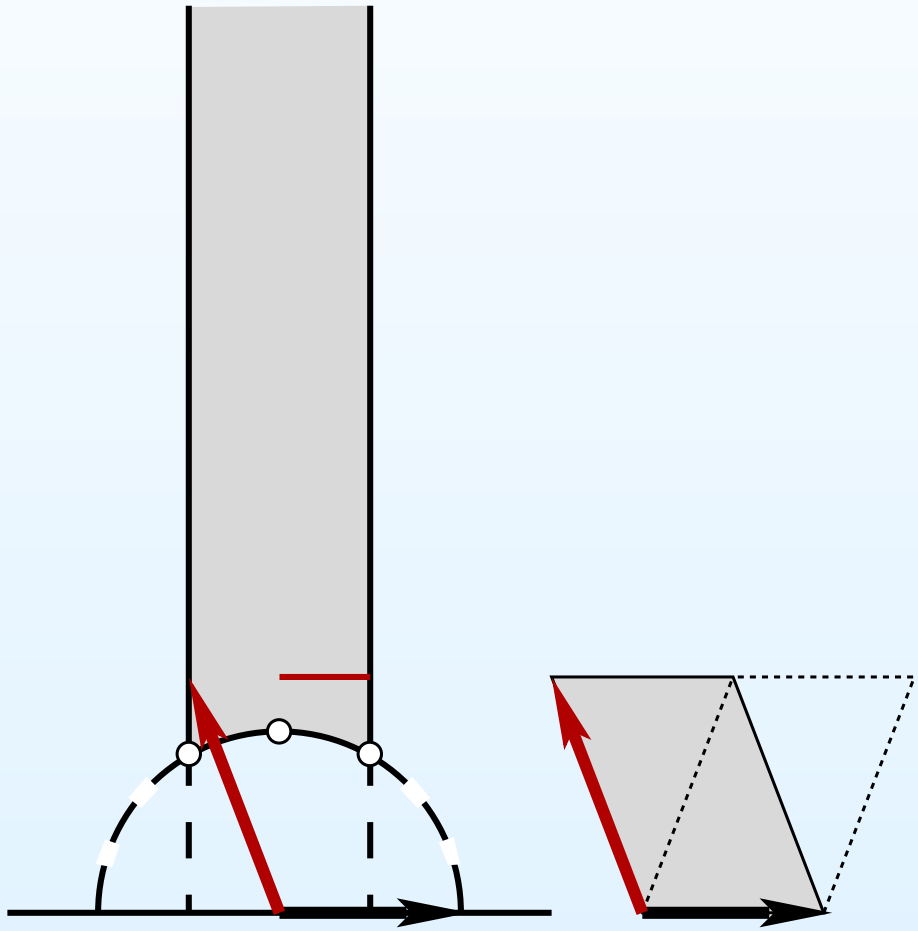

Closed horocycle in the moduli space of tori

Projection of a similar closed orbit of the *horocyclic flow* $\begin{pmatrix} 1 & t \\ 0 & 1 \end{pmatrix}$ to the moduli space of flat tori.

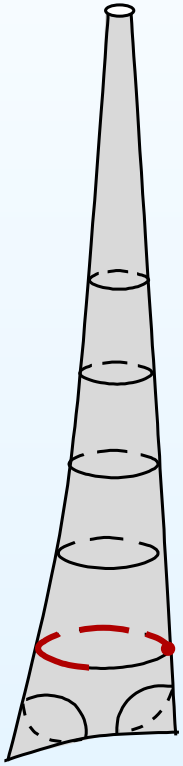

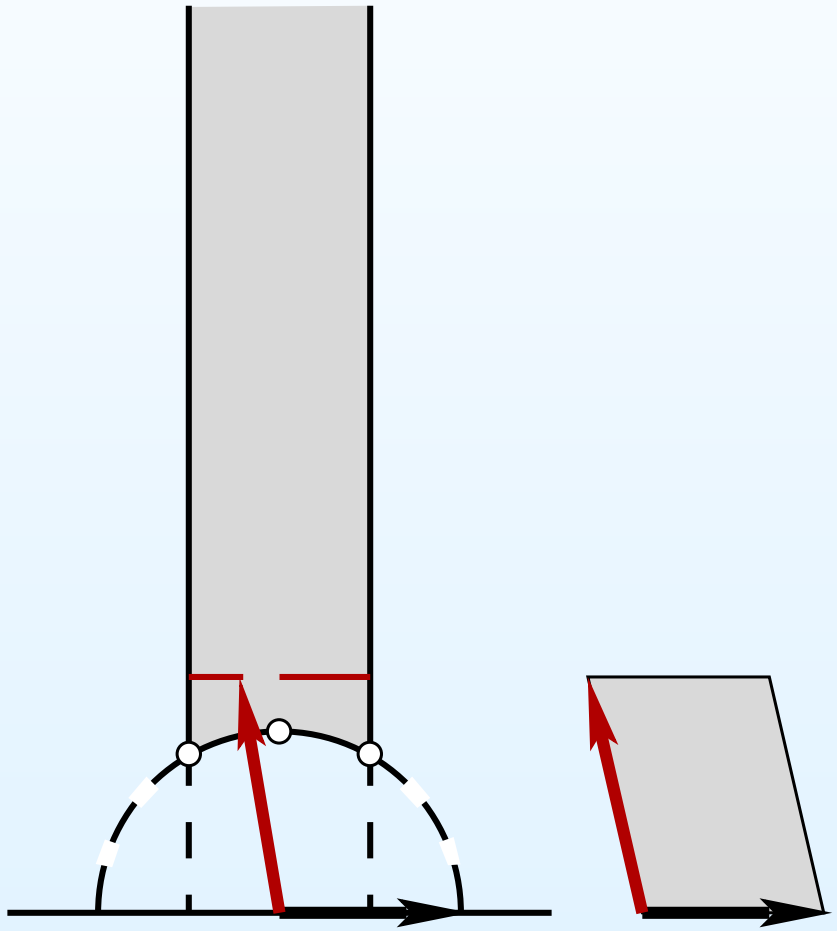

Closed horocycle in the moduli space of tori

Projection of a similar closed orbit of the *horocyclic flow* $\begin{pmatrix} 1 & t \\ 0 & 1 \end{pmatrix}$ to the moduli space of flat tori.

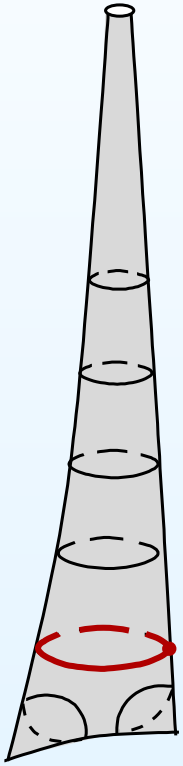

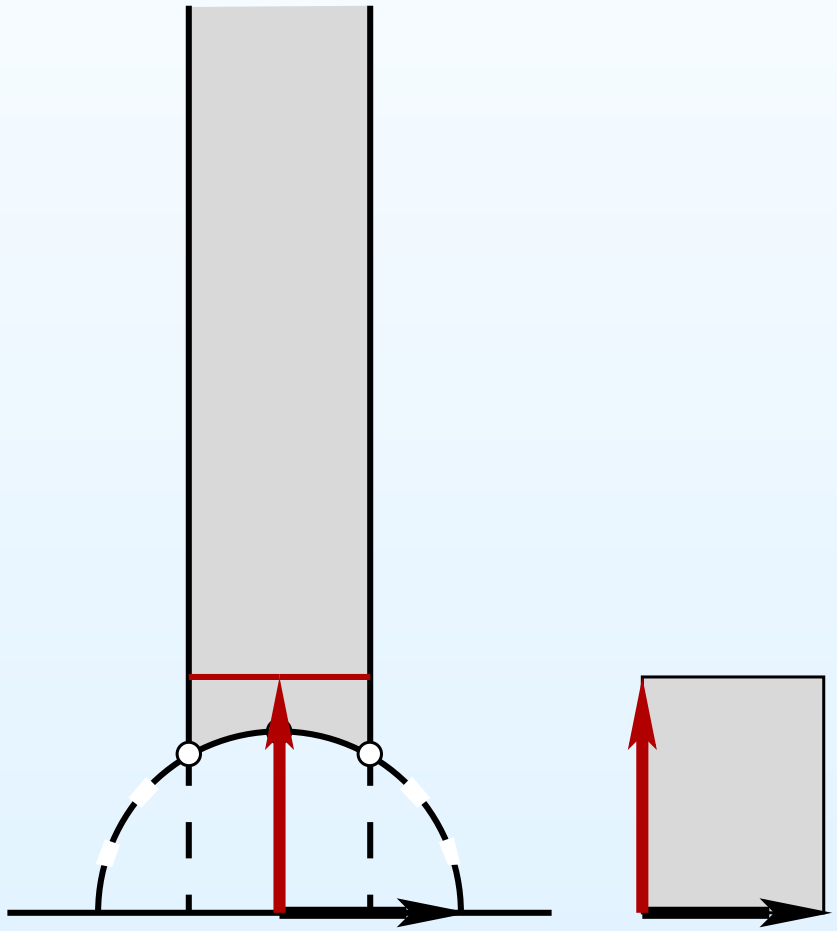

Pseudo-Anosov diffeomorphisms

Consider a composition of two Dehn twists $g = f_v \circ f_h =$

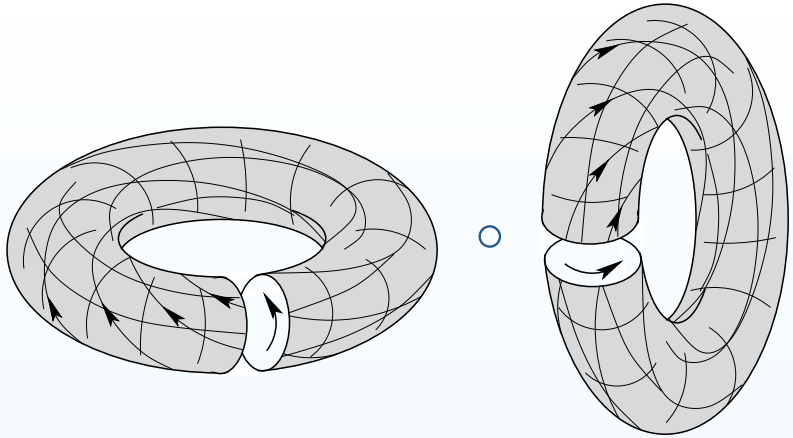

Pseudo-Anosov diffeomorphisms

Consider a composition of two Dehn twists $g = f_v \circ f_h =$

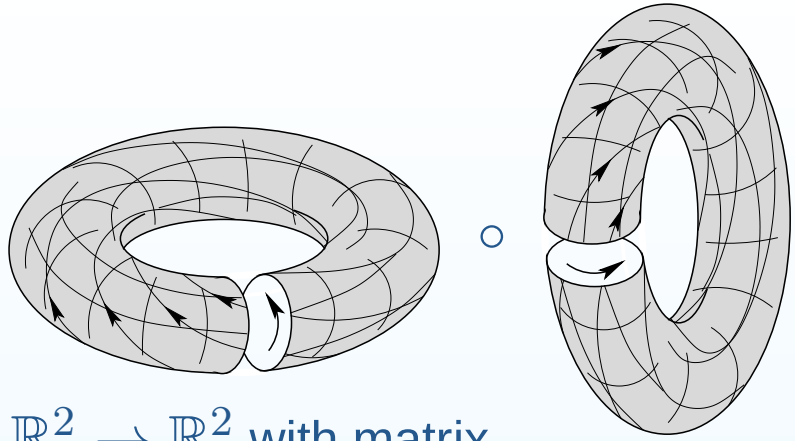

It corresponds to the integer linear map $\hat{g} : \mathbb{R}^2 \to \mathbb{R}^2$ with matrix $A = \begin{pmatrix} 1 & 1 \\ 1 & 2 \end{pmatrix} = \begin{pmatrix} 1 & 0 \\ 1 & 1 \end{pmatrix} \cdot \begin{pmatrix} 1 & 1 \\ 0 & 1 \end{pmatrix}$. Cutting and pasting appropriately the image parallelogram pattern we can check by hands that we can transform the new pattern to the initial square one.

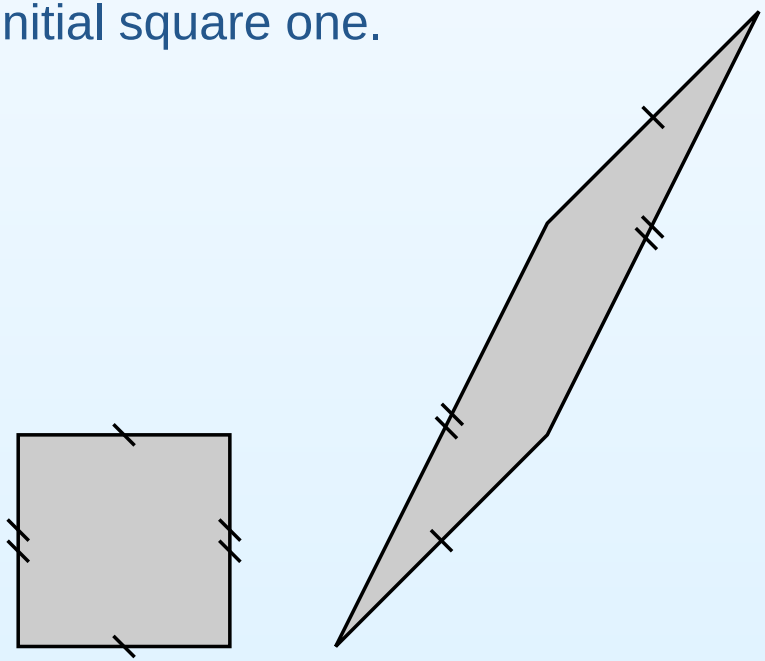

Pseudo-Anosov diffeomorphisms

Consider a composition of two Dehn twists $g = f_v \circ f_h =$

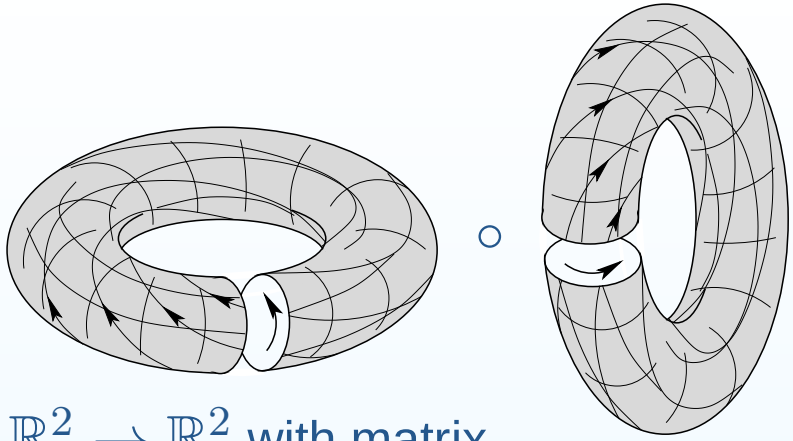

It corresponds to the integer linear map $\hat{g} : \mathbb{R}^2 \to \mathbb{R}^2$ with matrix $A = \begin{pmatrix} 1 & 1 \\ 1 & 2 \end{pmatrix} = \begin{pmatrix} 1 & 0 \\ 1 & 1 \end{pmatrix} \cdot \begin{pmatrix} 1 & 1 \\ 0 & 1 \end{pmatrix}$. Cutting and pasting appropriately the image parallelogram pattern we can check by hands that we can transform the new pattern to the initial square one.

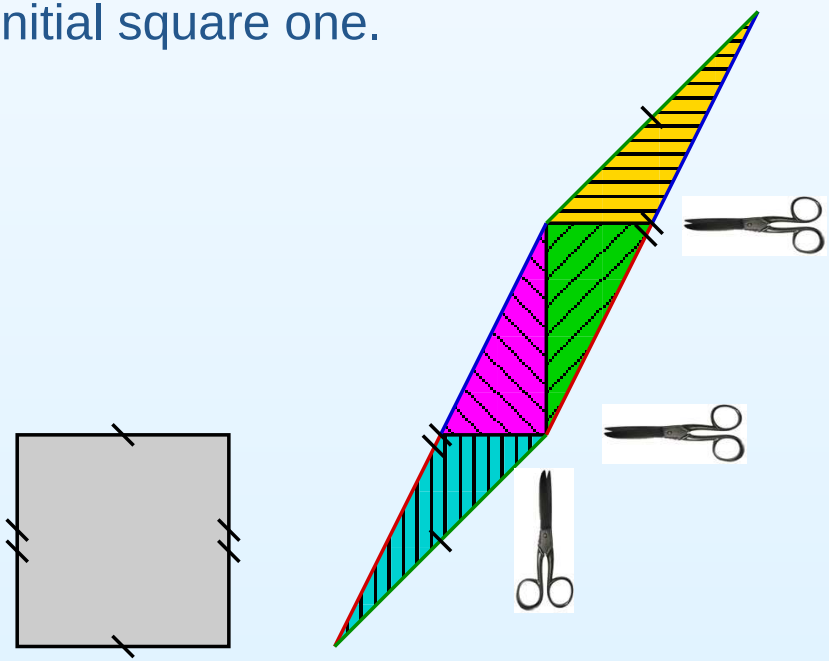

Pseudo-Anosov diffeomorphisms

Consider a composition of two Dehn twists $g = f_v \circ f_h =$

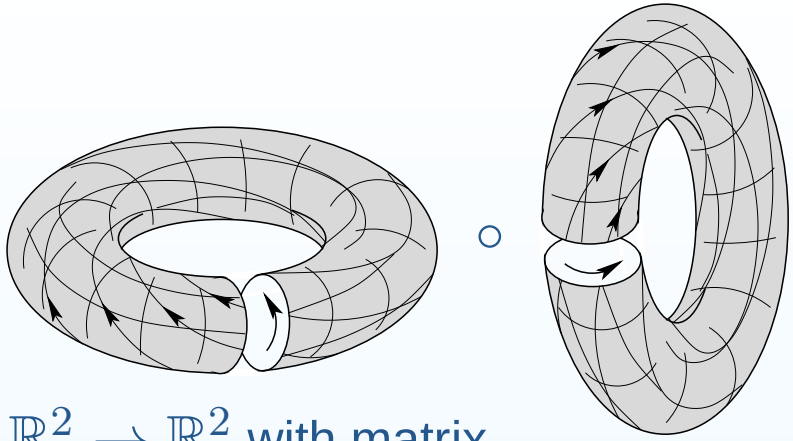

It corresponds to the integer linear map $\hat{g} : \mathbb{R}^2 \to \mathbb{R}^2$ with matrix $A = \begin{pmatrix} 1 & 1 \\ 1 & 2 \end{pmatrix} = \begin{pmatrix} 1 & 0 \\ 1 & 1 \end{pmatrix} \cdot \begin{pmatrix} 1 & 1 \\ 0 & 1 \end{pmatrix}$. Cutting and pasting appropriately the image parallelogram pattern we can check by hands that we can transform the new pattern to the initial square one.

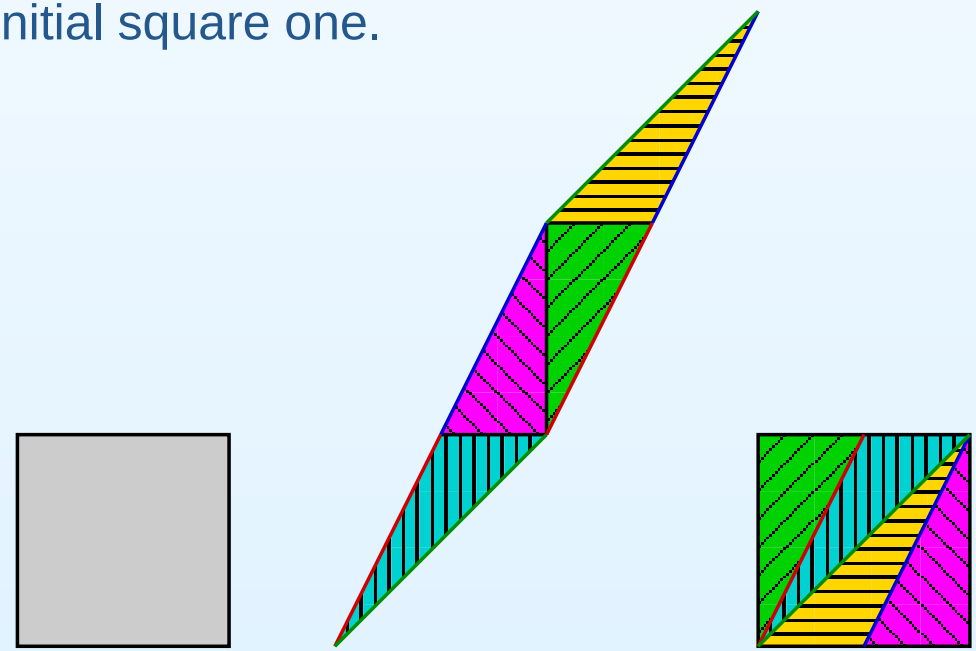

Closed geodesics in the space of tori

Consider eigenvectors $\vec{v}_{exp}$ and $\vec{v}_{contr}$ of the linear transformation $A = \begin{pmatrix} 1 & 1 \\ 1 & 2 \end{pmatrix}$ corresponding to the eigenvalues $\lambda > 1$ and to $1/\lambda < 1$ respectively. Consider two transversal foliations on the original torus in directions of $\vec{v}_{exp}$ and of $\vec{v}_{contr}$. We have just proved that expanding our torus $\mathbb{T}^2$ by factor λ in direction $\vec{v}_{exp}$ and contracting it by the factor λ in direction $\vec{v}_{contr}$ we get the original torus.

Closed geodesics in the space of tori

Consider eigenvectors $\vec{v}_{exp}$ and $\vec{v}_{contr}$ of the linear transformation $A = \begin{pmatrix} 1 & 1 \\ 1 & 2 \end{pmatrix}$ corresponding to the eigenvalues $\lambda > 1$ and to $1/\lambda < 1$ respectively. Consider two transversal foliations on the original torus in directions of $\vec{v}_{exp}$ and of $\vec{v}_{contr}$. We have just proved that expanding our torus $\mathbb{T}^2$ by factor λ in direction $\vec{v}_{exp}$ and contracting it by the factor λ in direction $\vec{v}_{contr}$ we get the original torus.

Consider a one-parameter family of flat tori obtained from the initial square torus by a continuous deformation expanding with a factor e^t in directions $\vec{v}_{exp}$ and contracting with a factor e^{-t} in direction $\vec{v}_{contr}$. By construction such one-parameter family defines a closed curve in the space of flat tori: after the time $t_0 = \log \lambda$ it closes up and follows itself.

One can check that this closed curve is, actually, a closed geodesics in the moduli spaces of tori.

Hodge bundle and Gauss–Manin connection

Consider a natural vector bundle over the stratum with a fiber $H^1(S;\mathbb{R})$ over a "point" (S,ω), called the *Hodge bundle*. It carries a canonical flat connection called *Gauss—Manin connection*: we have a lattice $H^1(S;\mathbb{Z})$ in each fiber, which tells us how we can locally identify the fibers. Thus, Teichmüller flow on $\mathcal{H}_1(d_1,\dots,d_n)$ defines Lyapunov exponents.

Hodge bundle and Gauss–Manin connection

Consider a natural vector bundle over the stratum with a fiber $H^1(S;\mathbb{R})$ over a "point" (S,ω), called the *Hodge bundle*. It carries a canonical flat connection called *Gauss—Manin connection*: we have a lattice $H^1(S;\mathbb{Z})$ in each fiber, which tells us how we can locally identify the fibers. Thus, Teichmüller flow on $\mathcal{H}_1(d_1,\dots,d_n)$ defines Lyapunov exponents.

Theorem (A. Eskin, M. Kontsevich, A. Z., 2014). *The Lyapunov exponents λ_i of the Hodge bundle $H^1_{\mathbb{R}}$ along the Teichmüller flow restricted to an $\mathrm{SL}(2,\mathbb{R})$-invariant suborbifold $\mathcal{L}\subseteq\mathcal{H}_1(d_1,\dots,d_n)$ satisfy:*

$$\lambda_1+\lambda_2+\dots+\lambda_g \;=\; \frac{1}{12}\cdot\sum_{i=1}^{n}\frac{d_i(d_i+2)}{d_i+1}+$$

$$\sum_{\substack{\text{Combinatorial types}\\ \text{of flat analogs}\\ \text{of stable curves}}}(\text{explicit combinatorial factor})\cdot\frac{\prod_{j=1}^{k}\operatorname{Vol}\mathcal{H}_1(\text{adjacent simpler strata})}{\operatorname{Vol}\mathcal{H}_1(d_1,\dots,d_n)}.$$

Renormalization applied to the wind-tree problem

We have reformulated the model problem of windtree billiard in terms of intersection indices $c(T) \circ h$ and $c(T) \circ v$ of a cycle $c(T)$ obtained by closing up a very long piece of vertical trajectory with two given cycles h and v on a given translation surface S.

Idea: apply the Teichmüller geodesic flow to S for an appropriate time t to get a flat surface $g_t S$ located very close to the original surface S. Close up the corresponding segment of the Teichmüller geodesic to get an associated pseudo-Anosov diffeomorphism $f : S \to S$.

Note that g_t exponentially contracts the vertical direction. Choosing $t \simeq \log T$ we can transform the very long cycle $c(T)$ to an ordinary integer cycle $f_* c(T)$ of length comparable to 1.

Conclusion: to compute $c(T) \circ h = f_* c(T) \circ f_* h$ we have to figure out how the pseudo-Anosov diffeomorphism f corresponding to a very long piece of a Teichmüller geodesic twists the distinguished cycles h and v. In other words, we have to compute the *Lyapunov exponents* for the cycles cycles h and v.

Windtree flat surface

Taking four copies of our $\mathbb{Z}^2$-periodic windtree billiard we can unfold it to a foliation on a $\mathbb{Z}^2$-periodic surface. Taking a quotient over $\mathbb{Z}^2$ we get a compact surface endowed with a measured foliation. Vertical and horizontal displacement (and thus, the diffusion) of billiard trajectories is described by the intersection numbers $c(t) \circ h$ and $c(t) \circ v$ of the cycle $c(t)$ obtained by closing up a long piece of leaf with a "parallel" h and a "meridian" v. Here $h = h_{00} + h_{10} - h_{01} - h_{11}$ and $v = v_{00} - v_{10} + v_{01} - v_{11}$.

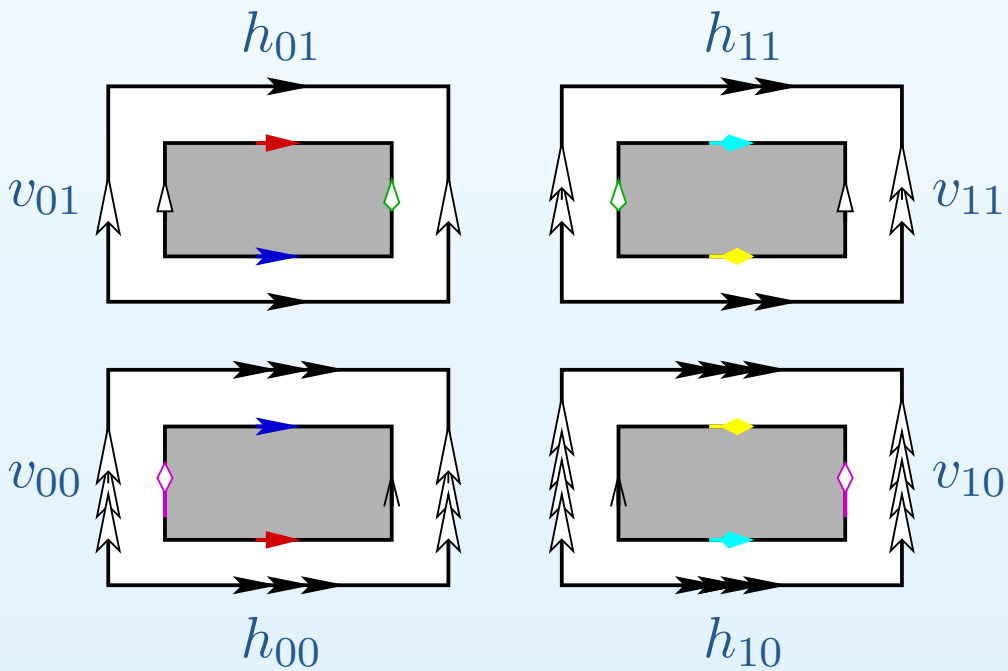

Solution of the windtree problem

Solution of the windtree problem

Theorem (J. Chaika–A. Eskin, 2014). *For any flat surface S almost all vertical directions define a Lyapunov-generic point in the orbit closure $\overline{\mathrm{SL}(2,\mathbb{R})\cdot S}$.*

Schematic solution of a generalized windtree problem

1. Find the family of flat surfaces $\mathcal{B}$ associated to the original family of rational billiards;
2. Find the orbit closure $\mathcal{L} = \overline{\mathrm{SL}(2,\mathbb{R})\cdot\mathcal{B}}$ of $\mathcal{B}$ inside the ambient moduli space (stratum).
3. Compute or estimate the relevant Lyapunov exponents of the Hodge bundle along the Teichmüller geodesic flow on $\mathcal{L}$.

Currently we do not have a slightest idea on how to approach the problem when the periodic obstacles are irrational.

Solution of the windtree problem

Theorem (J. Chaika–A. Eskin, 2014). *For any flat surface S almost all vertical directions define a Lyapunov-generic point in the orbit closure $\overline{\mathrm{SL}(2,\mathbb{R})\cdot S}$.*

Schematic solution of a generalized windtree problem

1. Find the family of flat surfaces $\mathcal{B}$ associated to the original family of rational billiards;
2. Find the orbit closure $\mathcal{L} = \overline{\mathrm{SL}(2,\mathbb{R})\cdot\mathcal{B}}$ of $\mathcal{B}$ inside the ambient moduli space (stratum).
3. Compute or estimate the relevant Lyapunov exponents of the Hodge bundle along the Teichmüller geodesic flow on $\mathcal{L}$.

Currently we do not have a slightest idea on how to approach the problem when the periodic obstacles are irrational.

Solution of the windtree problem

Theorem (J. Chaika–A. Eskin, 2014). *For any flat surface S almost all vertical directions define a Lyapunov-generic point in the orbit closure $\overline{\mathrm{SL}(2,\mathbb{R})\cdot S}$.*

Schematic solution of a generalized windtree problem

1. Find the family of flat surfaces $\mathcal{B}$ associated to the original family of rational billiards;
2. Find the orbit closure $\mathcal{L} = \overline{\mathrm{SL}(2,\mathbb{R})\cdot \mathcal{B}}$ of $\mathcal{B}$ inside the ambient moduli space (stratum).
3. Compute or estimate the relevant Lyapunov exponents of the Hodge bundle along the Teichmüller geodesic flow on $\mathcal{L}$.

Currently we do not have a slightest idea on how to approach the problem when the periodic obstacles are irrational.

Solution of the windtree problem

Theorem (J. Chaika–A. Eskin, 2014). *For any flat surface S almost all vertical directions define a Lyapunov-generic point in the orbit closure $\overline{\mathrm{SL}(2,\mathbb{R})\cdot S}$.*

Schematic solution of a generalized windtree problem

1. Find the family of flat surfaces $\mathcal{B}$ associated to the original family of rational billiards;
2. Find the orbit closure $\mathcal{L} = \overline{\mathrm{SL}(2,\mathbb{R})\cdot\mathcal{B}}$ of $\mathcal{B}$ inside the ambient moduli space (stratum).
3. Compute or estimate the relevant Lyapunov exponents of the Hodge bundle along the Teichmüller geodesic flow on $\mathcal{L}$.

Currently we do not have a slightest idea on how to approach the problem when the periodic obstacles are irrational.

Question. *What diffusion rate has a windtree billiard with "generic" (in any reasonable sense) irrational polygonal obstacles? Is it, by any chance, $\frac{1}{2}$?*

Changing the shape of the obstacle

Theorem (V. Delecroix, A. Z., 2015). *Changing the shape of the obstacle we get a different diffusion rate. Say, for a symmetric obstacle with $4m-4$ angles $3\pi/2$ and $4m$ angles $\pi/2$ the diffusion rate is*

$$\frac{(2m)!!}{(2m+1)!!} \sim \frac{\sqrt{\pi}}{2\sqrt{m}} \quad \text{as } m \to \infty\,.$$

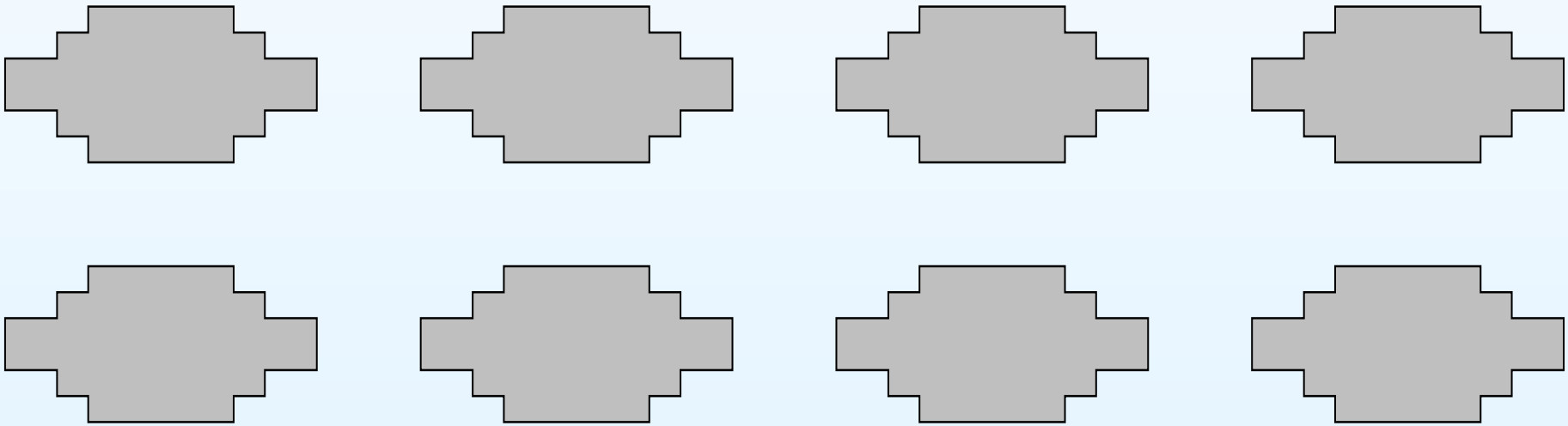

Note that once again the diffusion rate depends only on the number of the corners, but not on the (almost all) lengths of the sides, or other details of the shape of the obstacle.

Changing the shape of the obstacle

Theorem (V. Delecroix, A. Z., 2015). *Changing the shape of the obstacle we get a different diffusion rate. Say, for a symmetric obstacle with $4m-4$ angles $3\pi/2$ and $4m$ angles $\pi/2$ the diffusion rate is*

$$\frac{(2m)!!}{(2m+1)!!} \sim \frac{\sqrt{\pi}}{2\sqrt{m}} \quad \text{as } m \to \infty\,.$$

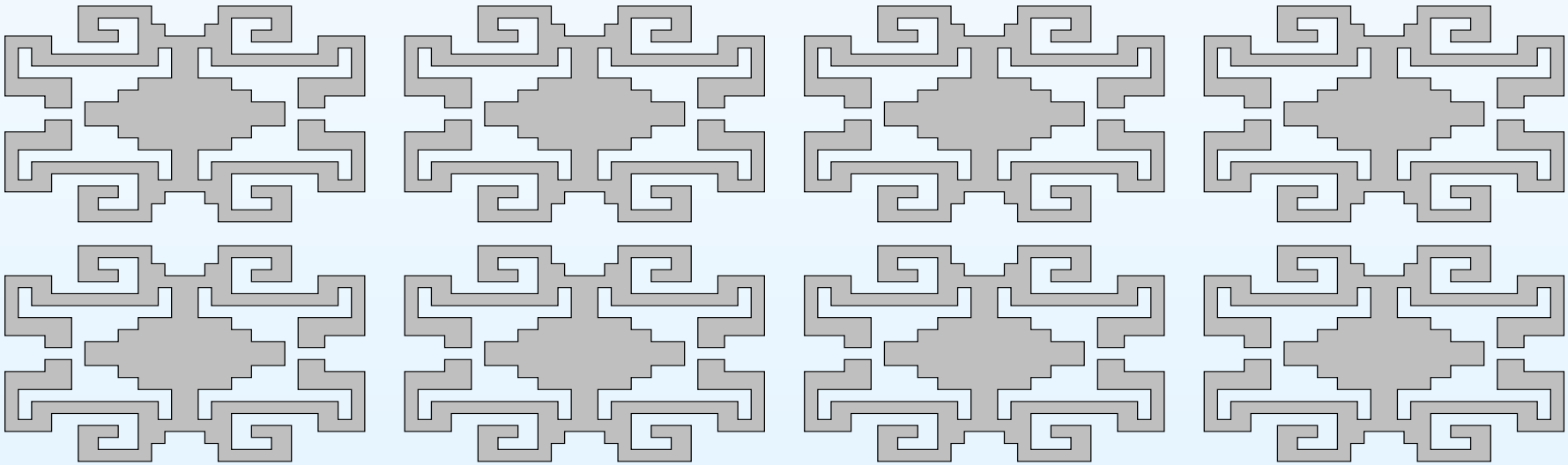

Note that once again the diffusion rate depends only on the number of the corners, but not on the (almost all) lengths of the sides, or other details of the shape of the obstacle.

Removing part of the obstacles

How would change the diffusion rate if we remove periodically one out of four obstacles in every 2×2 group of squares?

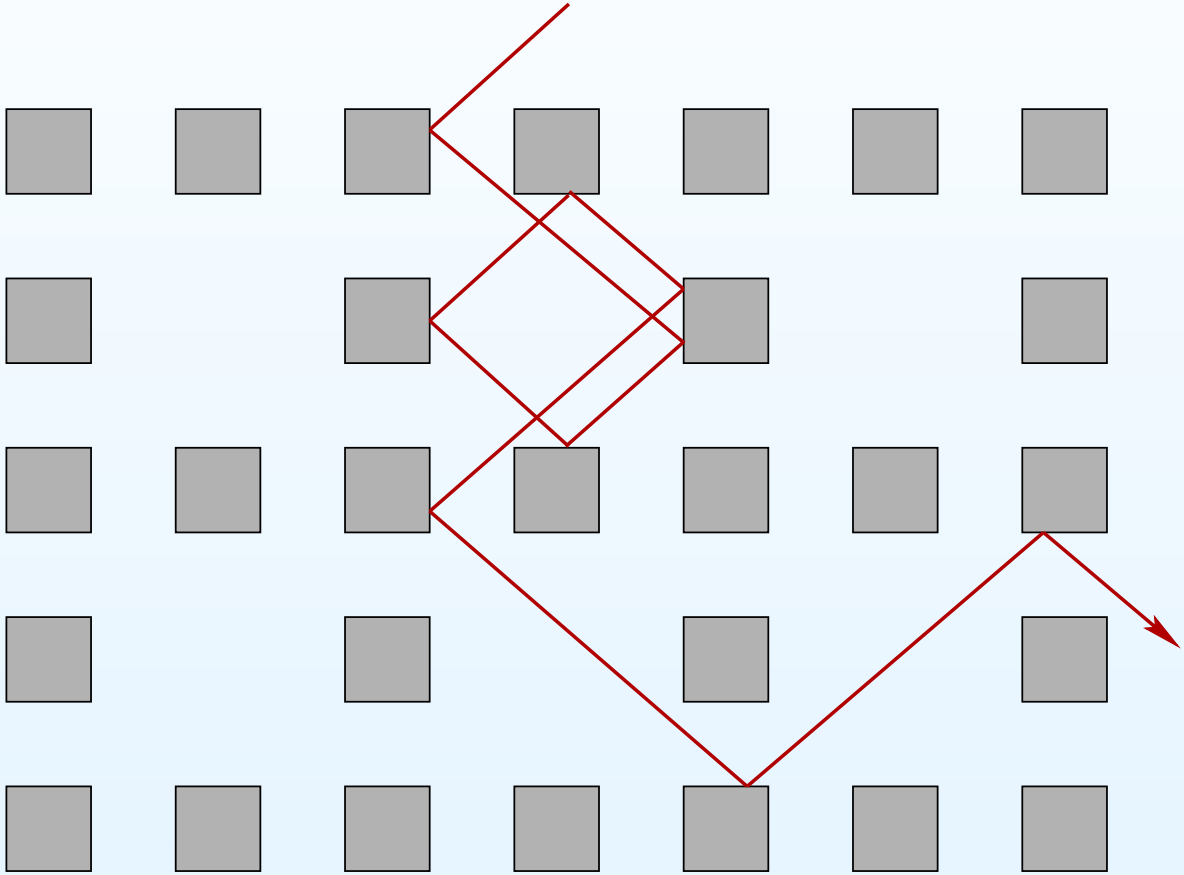

Removing part of the obstacles

How would change the diffusion rate if we remove periodically one out of four obstacles in every 2×2 group of squares?

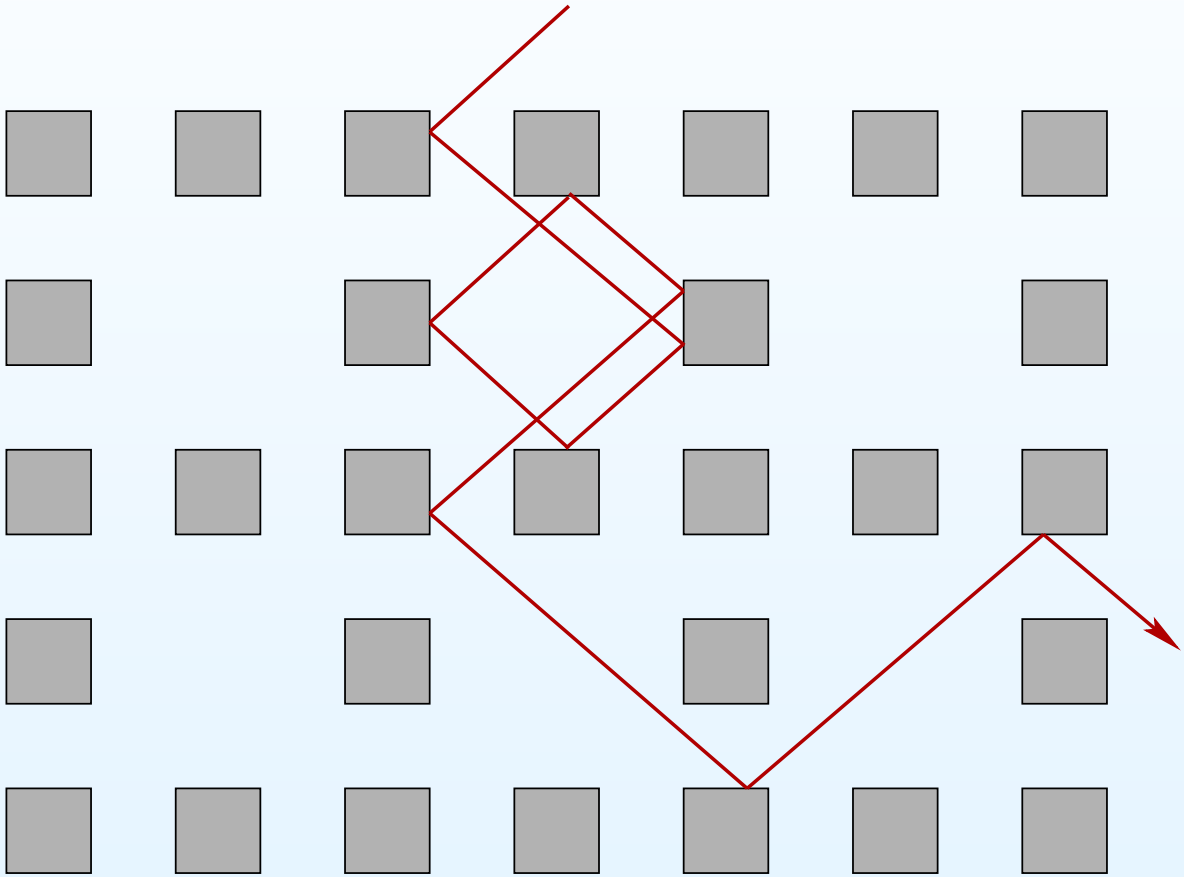

Lemma (V. Delecroix, A. Z., 2015). *Diffusion rate* $= \dfrac{491}{1053}$.

Removing part of the obstacles

And what about removing periodically two obstacles in every 2×2 group?

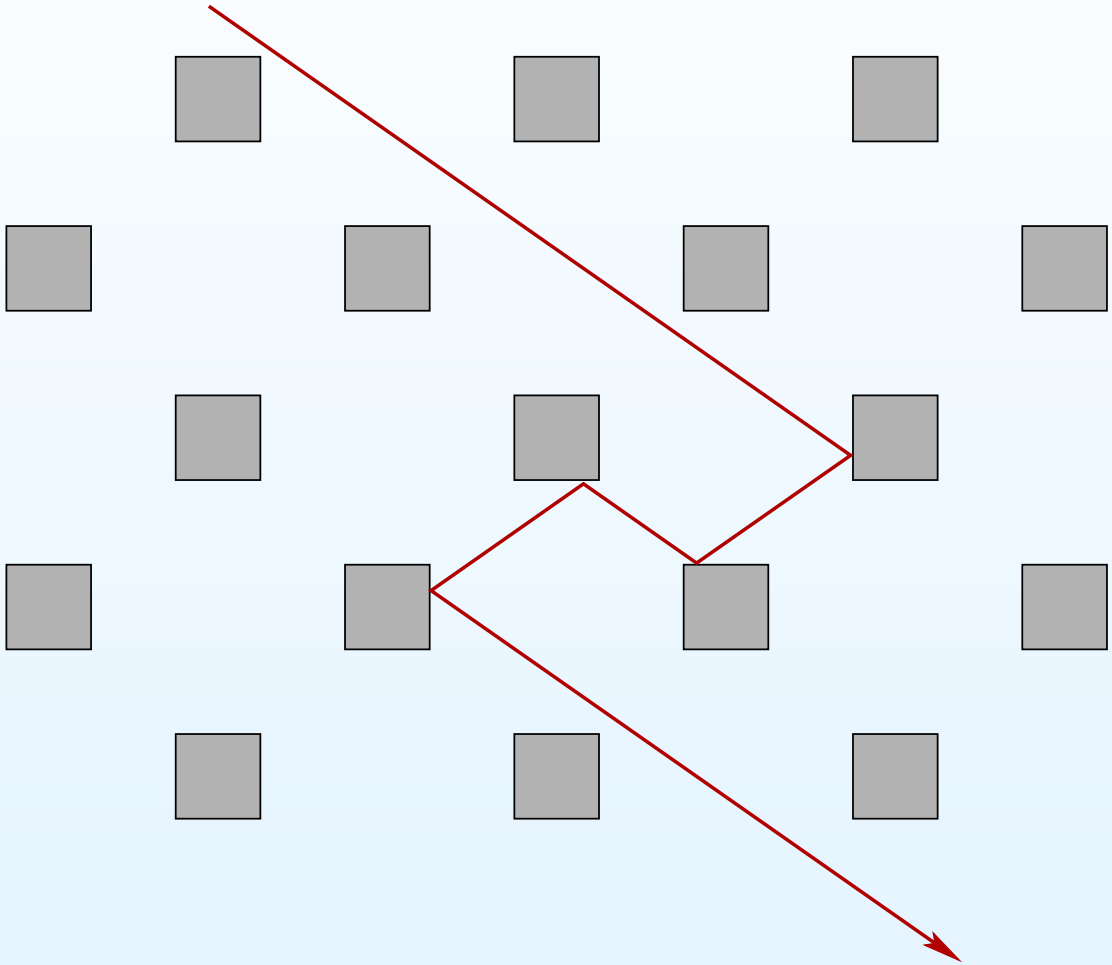

Removing part of the obstacles

And what about removing periodically two obstacles in every 2×2 group?

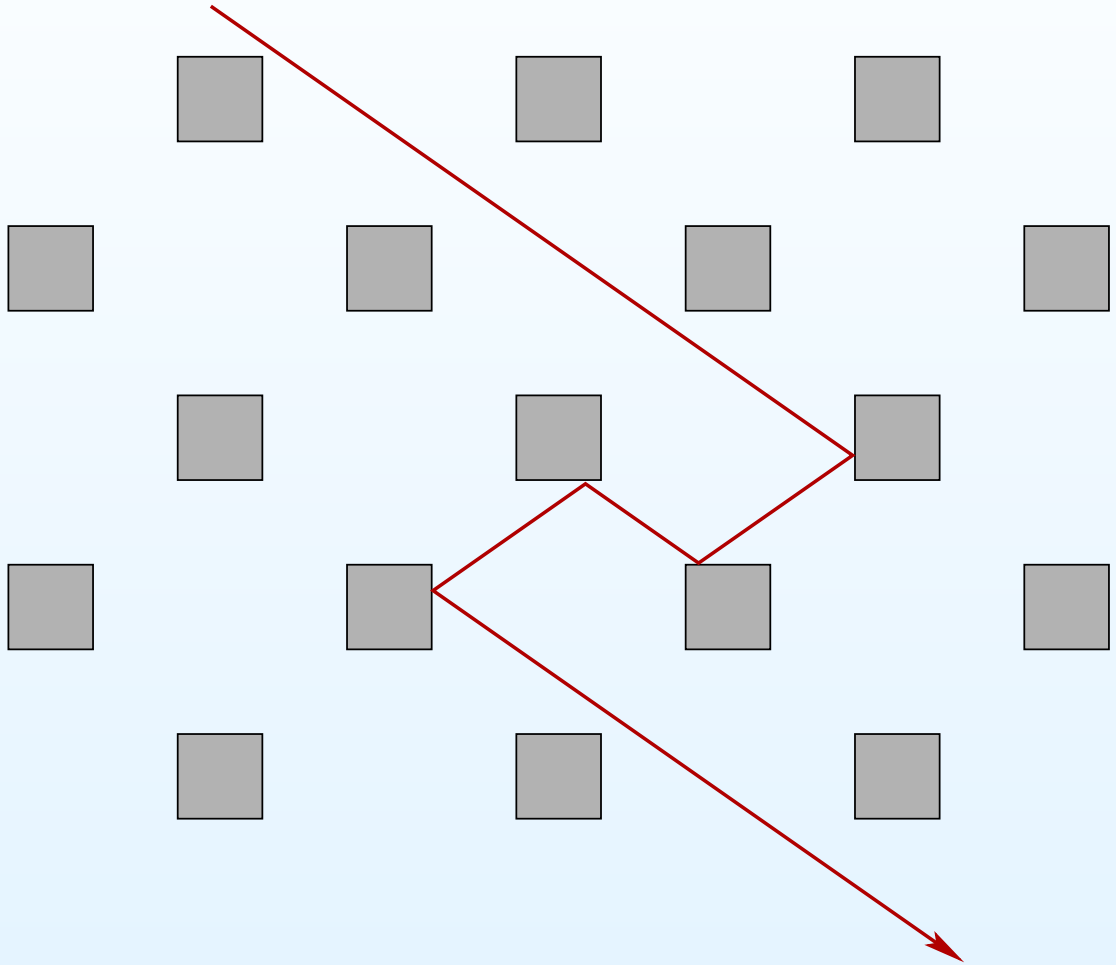

Lemma (V. Delecroix, A. Z., 2015). *Diffusion rate* $= \frac{2}{3}$.

Generic windtree model of high complexity

Theorem (Fougeron'20). *The diffusion rate of a periodic billiard with $n \geq 2$ random rectangular obstacles placed as in the picture equals the top Lyapunov exponent $\lambda_1^+(\mathcal{Q}_{n+1})$ of the Kontsevich–Zorich cocycle over the moduli space of holomorphic quadratic differentials of genus $g = n + 1$.*

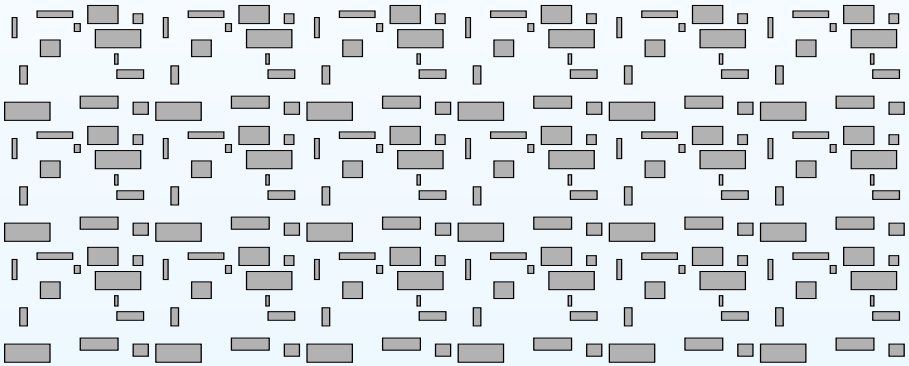

Conjectures (Zorich'98, Delecroix'15, Fougeron'19).

$$\lambda_2(\mathcal{H}(m_1, \ldots, m_n)) \to \frac{1}{2} \qquad \lambda_1^+(\mathcal{Q}(d_1, \ldots, d_n)) \to \frac{1}{2} \quad \text{as } g \to +\infty$$

uniformly for all $m_1 + \cdots + m_n = 2g - 2$ and $d_1 + \cdots + d_n = 4g - 4$.

The conjecture is confirmed by extensive computer experiments. Conceptually, it indicates that *parabolic* dynamical systems of large complexity in certain aspects mimic *hyperbolic* dynamical systems. For hyperelliptic strata we have $\lambda_2(\mathcal{H}_g^{hyp}) \to 1$ (Eskin–Kontsevich–Möller–Zorich + Fei Yu'18).

Computation of diffusion rate

1. Find a surface S endowed with a flat metric with conical singularities associated to the original *rational* periodic polygonal billiard. (Straightforward).

2. The surface S represents a point in the moduli space. Find an orbit closure $\mathcal{L} = \overline{\mathrm{GL}(2,\mathbb{R}) \cdot S}$ of S inside an ambient stratum in the moduli space. Uses very recent highly elaborated technology based on Eskin–Mirzakhani Magic Wand rigidity theorem. (Difficult, but in many cases doable due to works of P. Apisa, J. Chaika, C. McMullen, M. Mirzakhani, R. Mukamel, A. Wright, . . . , and due to a computer assisted tool currently developped by V. Delecroix–A. Eskin–J. Rüth–A. Wright incorporating all known tools.)

3. Compute or estimate the relevant Lyapunov exponent of the Hodge bundle along the Teichmüller geodesic flow on $\mathcal{L}$ (i.e. compute mean monodromy of the Hodge bundle along Teichmüller geodesics). (Currently can be done only in very special cases admitting extra symmetries leading to an equivariant splitting of the Hodge bundle. In these cases Eskin–Kontsevich–Zorich formula for the sum of the Lyapunov exponents is applicable to subbundles.)

We aim to advance in the last point in large genus *beyond symmetric cases*.